

**M. S. HAJ-ABED**

**Engineering of Hyperbranched Polyethylene and its Future  
Applications**

**By**

**MOHAMMAD HAJ-ABED**

**B. ENG.**

**A Thesis**

**Submitted to the School of Graduate Studies**

**in Partial Fulfillment of the Requirements**

**for the Degree**

**Master of Applied Science**

**McMaster University**

**© Copyright by Mohammad Haj-Abed, May, 2008**



## ABSTRACT

The present study is concerned with the modification of hyperbranched polyethylene (HBPE) via peroxide initiation and grafting with maleic anhydride. High-temperature solution modification using xylene as solvent was conducted, and the resultant material was characterized in terms of its structural, rheological, and physical properties, and compared to its unmodified counterpart. Moreover, the susceptibility of hyperbranched polyethylene to degradation/ crosslinking is investigated and compared to other commercially available polyolefins. Nevertheless, crosslinking of maleic anhydride grafted hyperbranched polyethylene is conducted in exploration of potential applications for this material.

Peroxide initiated modification of hyperbranched polyethylene was conducted to examine its vulnerability to degradation/ crosslinking relative to other commercially available polyolefins. Creep recovery was used to measure the percentage change in zero shear viscosity upon modification while  $^{13}\text{C}$ -NMR was used to give the number of methyl, methylene, and methane groups. The work elucidated that the dominant reaction undergone by hyperbranched polyethylene upon peroxide initiated modification is degradation, in a fashion similar to polypropylene, which is due to its high degree of branching.

Peroxide initiated grafting of hyperbranched polyethylene with maleic anhydride was conducted and the effects of reaction time, reaction temperature, monomer concentration, initiator type, and initiator concentration were systematically examined. The structure of the resultant functionalized polymer was confirmed via FTIR and  $^{13}\text{C}$ -NMR, and a maximal grafting density of 1.7 % was achieved using 2 wt.% MAH and 2 wt.% DCP in the preparation process. Alternating dominance between the grafting reaction and other side reactions was noticeable when varying the initiator and the monomer concentrations. Moreover, a drop in the water contact angle upon modification suggested that the grafted polymer is more compatible with polar substrates. Furthermore, rheological characterizations showed that functionalized HBPE exhibits a Newtonian behavior, which is characteristic of its unmodified counterpart; however showed some slight shear thinning behavior at low temperatures.

Crosslinking of HBPE-g-MAH using a diamine was conducted in solution and in melt in an effort to find a potential application for the resultant polymer. The structure of the resultant polymer was confirmed through FTIR and the effect of reaction time, reaction temperature, and diamine concentration on the degree of crosslinking was investigated. A maximal degree of crosslinking of 70% was achieved, where the structure of the polymer was found to have tremendous effect on the concentration of diamine necessary to gel the polymer. Nonetheless, the formation of a soft solid material from two liquid reactants suggested that HBPE-g-MAH could be a potential material for reaction injection molding applications.

## ACKNOWLEDGEMENT

I would like to start by expressing my sincere gratitude to the Almighty, where in His name, the most gracious, the most merciful, all good things start. I will next list a number of people who I am thankful to; and I apologize to those I forgot or could not mention.

I would like to express my sincere gratitude to my supervisor Dr. Shiping Zhu and my co-supervisor Dr. Santiago Faucher, for giving me the opportunity to pursue my degree and for their continuous support and guidance throughout my work. It has been indeed an honor to have them as my supervisors, where they showed great understanding, patience and encouragement. Also, I would like to thank my committee members, Dr. Michael Thompson and Dr. Gu Xu for taking the time to review my thesis and for being in my committee.

I would next like to thank my colleagues at McMaster University who helped me tremendously throughout the two years of the masters program, especially my group member who supported me throughout. I would also like to thank the faculty members of both the Chemical Engineering Department and Chemistry Department at McMaster University who helped me complete this thesis. Special thanks to my friends Adib Ternawly, Hani Badran, Omar Aker, Adnan Bin Mahfooz, Dana Aker, and Tala Abdulal for always being there for me.

Finally, I would like to express my deepest acknowledgements to my dear family: Mr. Sari Haj-Abed, Mrs. Wafa Rousan, Mr. Yazeed Haj-Abed, and Miss Farah Haj-Abed. They have been immensely supportive throughout my career life and a major factor to my success.

## TABLE OF CONTENTS

<b>Abstract</b>	<b>iii</b>
<b>Acknowledgment</b>	<b>v</b>
<b>Table of Contents</b>	<b>vii</b>
<b>List of Figures</b>	<b>xii</b>
<b>List of Tables</b>	<b>xviii</b>
<b>Nomenclature</b>	<b>xx</b>
<b>Chapter 1: Introduction, Research Background and Objectives</b>	
1.1    Introduction to Polyolefins and Their Production Technologies	1
1.1.1    Polypropylene	2
1.1.2    Polyethylene	4
1.2    Polyethylene with Controlled Chain Topology	6
1.2.1    Introduction	6
1.2.2    Hyperbranched Polyethylene Synthesis	9
1.3    Polymer Modification	11
1.3.1    Introduction	11
1.3.2    Modification by Grafting	11
1.3.3    Effect of Process Conditions	15
1.4    Thesis Research Objectives and Outlines	17
1.5    References	19

## Chapter 2: Peroxide Modification of Polyolefins

2.1	Introduction	22
2.1.1	Polymer Chemical Modification	22
2.1.2	Peroxide for Chemical Modification	24
2.1.3	<sup>13</sup> C-NMR Characterization	26
2.1.4	DEPT_135 Characterization	27
2.1.5	Determination of Zero Shear Viscosity from Creep-Recovery Experiments	28
2.1.6	Objective and Scope	30
2.2	Experimental	31
2.2.1	Materials	31
2.2.2	Peroxide Modification of Polyolefin	31
2.2.3	<sup>13</sup> C-NMR and DEPT_135 Sample Preparation	31
2.2.4	Disk Preparation	32
2.2.5	Rheological Characterization	32
2.3	Results and Discussion	33
2.3.1	<sup>13</sup> C-NMR Characterization of As Received and Modified Polyolefins	33
2.3.2	Correlation between Polymer Modification and Zero Shear Viscosity	39
2.4	Conclusion	41
2.5	References	42

### **Chapter 3: Maleic Anhydride Grafting of Hyperbranched Polyethylene**

3.1	Introduction	44
3.2	Experimental	45
3.2.1	Materials	45
3.2.2	HBPE-g-MAH Synthesis	46
3.2.3	Titration of Anhydride Content	46
3.2.4	FTIR Characterization	47
3.2.5	<sup>13</sup> C-NMR Characterization	47
3.2.6	Water Contact Angle Measurements	47
3.3	Results and Discussion	48
3.3.1	FTIR Characterization of Grafted Polymer	48
3.3.2	<sup>1</sup> H-NMR Characterization of Grafted Polymer	49
3.3.3	Effect of Initiator Type on Grafting Density	53
3.3.4	Effect of Reaction Temperature on Grafting Density	54
3.3.5	Effect of Initiator Concentration on Grafting Density	55
3.3.6	Effect of Monomer Concentration on Grafting Density	57
3.3.7	Water Contact Angle Results	58
3.4	Conclusion	59
3.5	References	60

### **Chapter 4: Rheological Characterization of HBPE and HBPE-g-MAH**

4.1	Introduction	62
4.1.1	Rheology	62

4.1.2	Theoretical Concepts in Rheology	63
4.1.3	Characterization of Liquids	64
4.1.4	Rheological Behavior of HBPE	68
4.1.5	Scope and Objective	69
4.2	Experimental	70
4.2.1	Materials	70
4.2.2	Rheological Characterization	70
4.3	Results and Discussion	71
4.3.1	Flow Curves for HBPE and HBPE-g-MAH	71
4.3.2	Oscillation Measurement Results for HBPE and HBPE-g-MAH	73
4.3.3	Creep-recovery Results for HBPE and HBPE-g-MAH	75
4.4	Conclusion	76
4.5	References	77

## **Chapter 5: Crosslinking of HBPE-g-MAH**

5.1	Introduction	78
5.1.1	Polymer Crosslinking	78
5.1.2	RIM History	79
5.1.3	RIM Operation	80
5.1.4	Advantages of RIM	81
5.1.5	Work Objective	82
5.2	Experimental	82

5.2.1	Materials	82
5.2.2	Solution Amination of HBPE-g-MAH	82
5.2.3	Melt Amination of HBPE-g-MAH	83
5.2.4	Gel Content Measurement	83
5.2.5	FTIR Characterization	83
5.3	Results and Discussion	84
5.3.1	FTIR Characterization of Crosslinked Polymer	84
5.3.2	Effect of Reaction Temperature on Degree of Crosslinking	84
5.3.3	Effect of Reaction Time on Degree of Crosslinking	85
5.3.4	Effect of Diamine Content on Degree of Crosslinking	87
5.3.5	Application to Reaction Injection Molding	90
5.4	Conclusion	93
5.5	References	94

## **Chapter 6: Significant Research Contributions and Recommendations for Future Developments**

6.1	Significant Research Contributions of Thesis Work	95
6.2	Recommendations for Future Research	97
6.2.1	Melt Grafting of Hyperbranched Polyethylene	97
6.2.2	Mechanical Testing and Characterization of Crosslinked HBPE-g-MAH	97
6.2.3	Reaction Injection Molding of HBPE-g-MAH	98

## List of Figures

### Chapter 1

Figure 1.1	Global polyolefin consumption.	1
Figure 1.2	Tacticity in polypropylene.	3
Figure 1.3	Schematic representation of the different classes of polyethylene. (a) High density polyethylene; (b) low density polyethylene; (c) linear low-density polyethylene.	5
Figure 1.4	Structures of dendrimers and hyperbranched polymers.	7
Figure 1.5	Properties and application of dendrimers and hyperbranched polymers.	8
Figure 1.6	Schematic for the possibility of formation of linear and hyperbranched polymers from metal based catalysts.	9
Figure 1.7	Schematic of the chain-walking mechanism.	10
Figure 1.8	Possible reaction of the grafting of PP with MAH.	13
Figure 1.9	Possible reaction of the grafting of PE with MAH.	14
Figure 1.10	Degradation mechanism of polypropylene.	14
Figure 1.11	Crosslinking mechanism of polyethylene.	15

### Chapter 2

Figure 2.1	Dicumyl peroxide decomposition mechanism.	25
Figure 2.2	Illustration of correlating DEPT spectra to a $^{13}\text{C}$ spectrum.	28
Figure 2.3	Illustration of creep-recovery results characteristic of elastic and viscous materials, respectively.	28

Figure 2.4	Strain vs. time curve obtained from creep-recovery experiment is shown. The slope of the creep curve is used in conjunction with the stress applied to calculate the respective shear rate viscosity.	30
Figure 2.5	Chain scission in PP.	34
Figure 2.6	Bimolecular recombination of backbone radicals in HBPE.	36
Figure 2.7	Radicals formed upon hydrogen abstraction from LDPE backbone.	36
Figure 2.8	Structures formed due to the recombination of radicals in LDPE.	37
Figure 2.9	Radical addition to vinyl groups in LDPE.	37
Figure 2.10	Percentage change in zero shear viscosity for various polyolefin grades before and after modification. Rheological characterization was conducted 10-20 °C above the melting temperature of each polyolefin, and experiments were conducted at 10 °C intervals. Negative changes in viscosity identify degradation as opposed to crosslinking, which is characterized by positive changes.	40

### Chapter 3

Figure 3.1	Infrared spectrum of HBPE-g-MAH in the range 1700 to 1900 $\text{cm}^{-1}$ prepared using 2 wt.% MAH, 2 wt.% DCP, and a reaction time of 1 hr at 130 °C. 24 scans were acquired with a resolution of 4 $\text{cm}^{-1}$ .	49
Figure 3.2	$^1\text{H-NMR}$ of HBPE-g-MAH prepared using 2 wt.% DCP and 2 wt.% MAH at 130 °C for 1 hr.	50

Figure 3.3	<sup>1</sup> H-NMR of HBPE-g-MAH prepared using 2 wt.% DCP and 2 wt.% MAH at 130 °C for 1 hr.	50
Figure 3.4	Structure formula representing the methyne and two methylene protons of the succinic anhydride ring grafted on the polymer backbone.	51
Figure 3.5	Reaction route for the formation of the graft structure displayed in Figure 3.4.	51
Figure 3.6	Structure formula representing the two methylene protons of the succinic anhydride ring grafted on the polymer backbone.	52
Figure 3.7	Reaction route for the formation of the graft structure displayed in Figure 3.6.	52
Figure 3.8	Structure formula showing the two hydrogens at the chains end of the succinyl terminated HBPE.	53
Figure 3.9	Effect of reaction temperature on grafting density. The reaction was conducted using 2 wt.% DCP, 2 wt.% MAH, and xylene solvent for 1 hr under a nitrogen blanket. Temperatures in the range 110 – 130 °C were examined.	55
Figure 3.10	Effect of initiator concentration on grafting density and reaction efficiency. Reaction was conducted using dicumyl peroxide as an initiator, varying its concentration from 0 – 4 wt.%. Reaction was allowed to proceed for 1 hr, at 130 °C, under a nitrogen blanket using 2 wt.% MAH and xylene solvent.	56

Figure 3.11	Effect of maleic anhydride concentration on grafting density. Maleic anhydride concentration was varied in the range 0 – 4 wt.%. Reaction was conducted at 130 °C for 1 hr under a nitrogen blanket, using 2 wt.% DCP, and xylene solvent.	58
-------------	--	----

## Chapter 4

Figure 4.1	Schematic illustrating the link between rheological parameters and the molecular structure and processing behavior of a material.	63
Figure 4.2	Typical flow and viscosity curves of a Newtonian material.	65
Figure 4.3	Typical viscosity and flow curves of a shear thinning material.	66
Figure 4.4	Typical viscosity and flow curves of a shear thickening material.	67
Figure 4.5	Steady shear viscosity as a function of shear rate for HBPE prepared at 35 °C, and 0.2 atm, using a Pd-diimine catalyst, measured at various temperatures.	69
Figure 4.6	Steady shear viscosity as a function of shear rate for HBPE, measured at various temperatures in the range 25- 65 °C.	71
Figure 4.7	Steady shear viscosity as a function of shear rate for HBPE-g-MAH, measured at various temperatures in the range 25- 65 °C.	72
Figure 4.8	Complex viscosity as a function of frequency for HBPE, measured at various temperatures in the range 25- 65 °C.	74
Figure 4.9	Complex viscosity as a function of frequency for HBPE-g-MAH, measured at various temperatures in the range 25- 65 °C.	74

Figure 4.10	Compliance curve for HBPE obtained from creep-recovery experiment, measured at various temperatures in the range 25- 65 °C.	75
Figure 4.11	Compliance curve for HBPE-g-MAH obtained from creep-recovery experiment, measured at various temperatures in the range 25- 65 °C.	76
 <b>Chapter 5</b>		
Figure 5.1	Reaction injection molding process schematic.	81
Figure 5.2	Infrared spectrum of diamine crosslinked HBPE-g-MAH between 1650 and 1850 $\text{cm}^{-1}$ crosslinked using 4 mol diamine/ mol HBPE-g-MAH, reaction time of 1 hr at 130 °C. 64 scans were acquired with a resolution of 4 $\text{cm}^{-1}$ .	84
Figure 5.3	Effect of reaction temperature on the degree of crosslinking of HBPE-g-MAH. The reaction was conducted by adding 4 mol diamine/ mol HBPE-g-MAH, using xylene as a solvent under a nitrogen blanket. Reaction time was 1 hr and temperature was varied in the range 110 – 130 °C.	85
Figure 5.4	Effect of reaction time on the degree of crosslinking for HBPE-g-MAH. Reaction was conducted by adding 4 mol diamine/ mol HBPE-g-MAH, using xylene as a solvent under a nitrogen blanket. Reaction temperature was 130 °C and reaction time was varied from 1 – 4 hrs.	86
Figure 5.5	Reaction of diamine with hyperbranched polyethylene.	88
Figure 5.6	Effect of diamine concentration on the degree of crosslinking of HBPE-g-MAH. Reaction was conducted at 130 °C for 1 hr using xylene as a solvent	

	under a nitrogen blanket. Diamine concentration was varied in the range 0	
	– 8 mol diamine/ mol HBPE-g-MAH.	89
Figure 5.7	Illustration for the amination reaction of (a) HBPE and (b) PP.	90
Figure 5.8	Process schematic for reaction injection molding.	91
Figure 5.9	Diamine crosslinked HBPE-g-MAH, prepared by using 4 mol diamine/ mol HBPE-g-MAH. Mixture was sonicated to achieve good mixing before conducting melt reaction at 180 °C for 1 hr.	92
Figure 5.10	Melt prepared diamine crosslinked HBPE-g-MAH, after finding the degree of gelation using a Soxhlet apparatus; 70% of the resultant polymer was gelled.	92

## List of Tables

### Chapter 1

Table 1.1	Effect of process conditions on side reaction and grafting yields.	16
-----------	--	----

### Chapter 2

Table 2.1	Survey of commercial peroxides.	26
Table 2.2	Number of CH, CH <sub>2</sub> , CH <sub>3</sub> , and vinylidene groups for unmodified and modified polyolefins. Results obtained by integrating the peaks in the <sup>13</sup> C-NMR spectra. Spectra obtained using a 30° pulse angle of 6 μs, an acquisition time of 1s, a preparation delay time of 2s, and 12,000 scans. Spectra recorded at 120 °C using 1,1,2,2-tetrachloroethane-d <sub>4</sub> as a solvent, and Cr(acac) <sub>3</sub> as a relaxation agent.	33

### Chapter 3

Table 3.1	Effect of type of initiator on grafting density and reaction efficiency. Dicumyl peroxide (DCP) and dibenzoyl peroxide (BPO) were used as initiators. Reaction conducted at 130 °C using 2 wt.% MAH, 2 wt.% initiator, xylene solvent, and allowed to proceed for 1 hr under a nitrogen blanket.	54
Table 3.2	Water contact angle results for HBPE, (2 wt.% DCP, 3 wt.% MAH) HBPE, and (2 wt.% DCP, 2 wt.% MAH) HBPE. Samples were prepared	

by casting a thin film onto a polyester film, applying a water droplet and measuring the water contact angle. 59

#### **Chapter 4**

Table 4.1 Definition of the most commonly used rheological terms. 63

## Nomenclature

AFM	Atomic force microscopy
Atm	Atmosphere(s)
BPO	Benzoyl peroxide
DCP	Dicumyl peroxide
DEPT	Distortionless Enhancement by Polarization Transfer
FTIR	Fourier Transform Infrared
GD	Grafting density (%)
HBPE	Hyperbranched polyethylene
HDPE	High density polyethylene
LCB	Long chain branch
LDPE	Low density polyethylene
LLDPE	Linear low density polyethylene
MAH	Maleic anhydride
NMR	Nuclear magnetic resonance
NOE	Nuclear Overhauser Enhancement
ppm	parts per million
PE	Polyethylene
PP	Polypropylene
PS	Polystyrene
PVC	Polyvinyl chloride
RIM	Reaction Injection Molding

SCB	Short chain branch
wt.	weight
$\theta$	pulse angle
$\eta$	viscosity
$\eta_0$	zero shear rate viscosity
$\gamma$	shear
$\dot{\gamma}$	shear rate
$\Delta\gamma$	change in strain
$\Delta t$	change in time
$\sigma$	stress
$\tau$	relaxation time

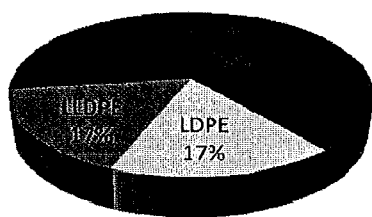
## Chapter 1: Introduction, Research Background and Objectives

### 1.1 Introduction to Polyolefins and Their Production Technologies

Polyolefin market behaviour has been greatly influenced by its global consumption, thus high consumption resulted in a growth rate exceeding five percent per year. This in turn led to the formation of an extremely commoditized industry, where all investment/ production decisions made were highly impacted by revenues and cost [1].

Polyolefins are categorized based on their structure and properties, where the main types fall under the umbrella of polyethylene (PE) and polypropylene (PP). Polyethylenes include linear low-density polyethylene (LLDPE), low-density polyethylene (LDPE), and high-density polyethylene (HDPE). Global polyolefins demand exceeded 111 million tons in 2006, however, Figure 1.1 shows that the demand is forecasted to rise to 200 million tons by 2020 [2].

**2006: 111 million tons**



**2020: 200 million tons**

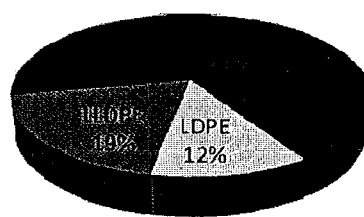


**Figure 1.1:** Global polyolefin consumption [2].

### 1.1.1 Polypropylene

Polypropylene is one of the most widely used polyolefins, where its world consumption has increased from 1.2 million tonnes in 1970 to 25 million tonnes in 1999. Nonetheless, forecasters expect a larger undiminished growth for this material [3]. Polypropylenes low density, 0.91-0.92 g/ml [4], makes it cheap on a volume basis compared to other polyolefins, and therefore it is widely used in the packaging, transport, appliance, furniture, and textile applications [3]. Its use in such industries is further induced by its versatility, especially in manufacturing injected, extruded, and fibrous products.

Dependent on the location of the methyl groups on a polypropylene chain produced by coordination polymerization, polypropylene is categorized as atactic, isotactic, or syndiotactic (Figure 1.2). Polypropylene is atactic when the methyl groups are distributed randomly on either side of the chain, isotactic when all the methyl groups are located on one side of the chain, and syndiotactic when the methyl groups alternate regularly on both sides of the chain.

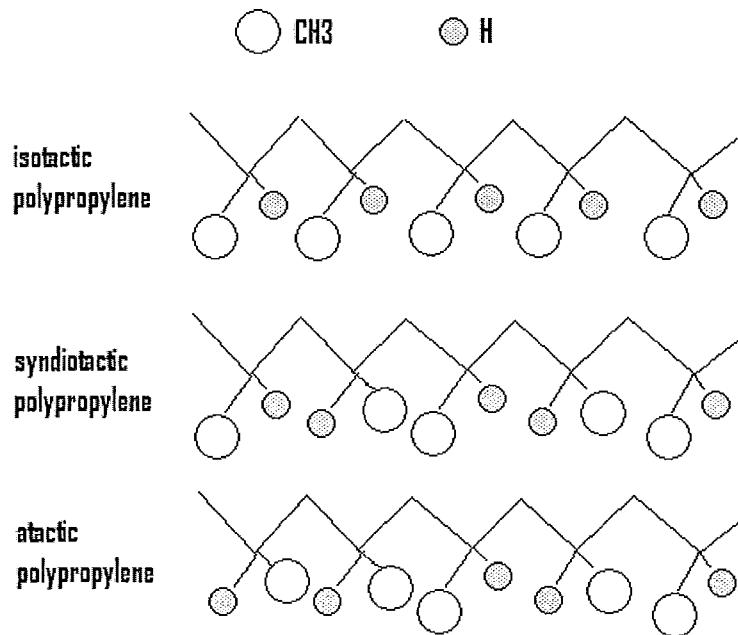


**Figure 1.2:** Tacticity in polypropylene [5].

### *Atactic Polypropylene*

Atactic polypropylene is synthesized using cationic polymerization, which gives it its waxy character. It represents only 2-3% of the world-wide produced polypropylene, and it was the only form of polypropylenes available until the development of the Ziegler-Natta catalysts. It is commonly used in additives, or in polymer blends [3].

### *Isotactic Polypropylene*

Isotactic polypropylene is commercially available in three forms: homopolymer, random copolymer, and block copolymer, respectively. Their physical properties range from higher strength and stiffness combined with reduced impact resistance to greater toughness accompanied by lower strength.

Propylene monomer with no other additives forms the homopolymer, which exhibits the highest melting point (165 °C) and stiffness of the three types, and is marketed with a wide range of melt flows. A random copolymer is produced by incorporating 0.5-3 wt.% ethylene monomer during polymerization, which produces a chain with decreased regularity, and enhanced flexibility. This in turn, reduces the crystallinity and modulus of the homopolymer, in addition to the melting point (145-150 °C) [3].

### *Syndiotactic Polypropylene*

Still in its early stages of development, however, compared to isotactic polypropylene, it has much better impact properties and clarity albeit its lack of stiffness. Its primary application would be in the packaging industry [3].

#### 1.1.2 Polyethylene

Polyethylene dominates the global thermoplastic market, accounting for around 47 million tonnes in 1999 [3]. The conventional way of categorizing the polyethylene is based on the density and linearity of the final product, where the three main classes of polyethylene are low-density polyethylene (LDPE), linear low-density polyethylene (LLDPE), and high-density polyethylene (HDPE), which are displayed in Figure 1.3.

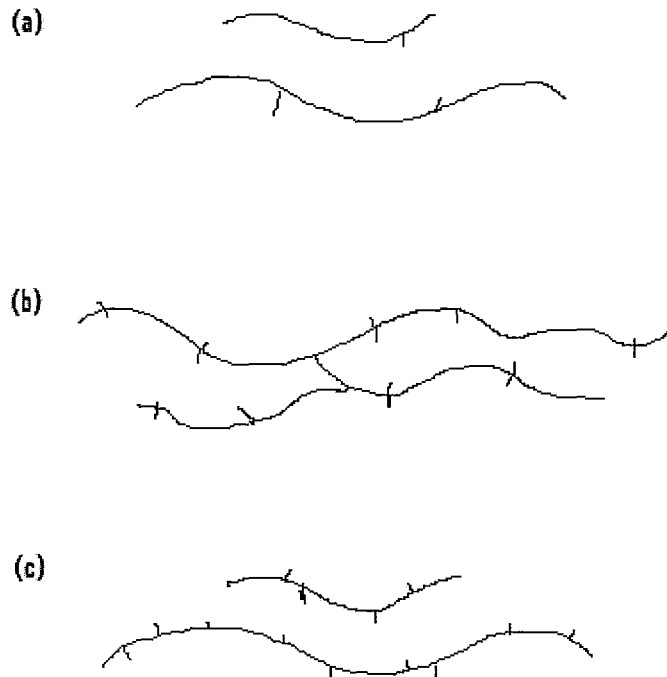


**Figure 1.3:** Schematic representation of the different classes of polyethylene. (a) High density polyethylene; (b) low density polyethylene; (c) linear low-density polyethylene [6].

### ***Low Density Polyethylene***

Low-density polyethylene is a highly branched homopolymer formed of short chain branches (SCB) generated by chain backbiting and long chain branches (LCB) generated by chain transfer to polymer. The coexistence of SCB and LSB gives low density polyethylene its low-density compared to other polyethylene materials, with a density in the range 0.910 to 0.935 g/ml. Controlling the molecular weight, molecular weight distribution, and crystallinity of the material, tailors it for different types of applications [3].

### ***Linear Low Density Polyethylene***

Linear low density polyethylene typically has a density ranging between 0.910 to 0.925 g/ml. It is essentially a linear polymer containing a controlled amount of short chain branches (SCB), formed by copolymerization of ethylene and small amount of  $\alpha$ -olefin, such as 1-butene, 1-hexene, and 1-octene [3].

### ***High Density Polyethylene***

High-density polyethylene is an ethylene homopolymer, which is linear in nature with no or very low levels of short chain branching, with a density ranging from 0.940 to 0.965 g/ml. The crystalline nature of high density polyethylene contributes to its high density, and therefore it can be used in various extrusion and molding applications [3].

## 1.2 Polyethylenes with Controlled Chain Topology

### 1.2.1 Introduction

Control of polymer chain topology and architecture is an important theme in polymer science, where the target is to produce specialty polymers with novel properties and applications. In the past two decades, many new concepts and unique synthetic routes have been developed to prepare polymers with different chain topologies and architectures, such as dendrimers [7], hyperbranched [8], and supramolecular polymers [9]. In spite of the advanced properties of the resultant polymers, most of the synthetic routes are costly, sophisticated, and involve multi-step synthesis, especially for dendrimers; due to the high regularity and uniformity needed within the produced polymer.



Although polycondensation has been used to prepare multiple hyperbranched polymers, there was no success in preparing hyperbranched polyethylene with different chain topologies from inexpensive ethylene monomer until chain-walking catalysts had been developed.

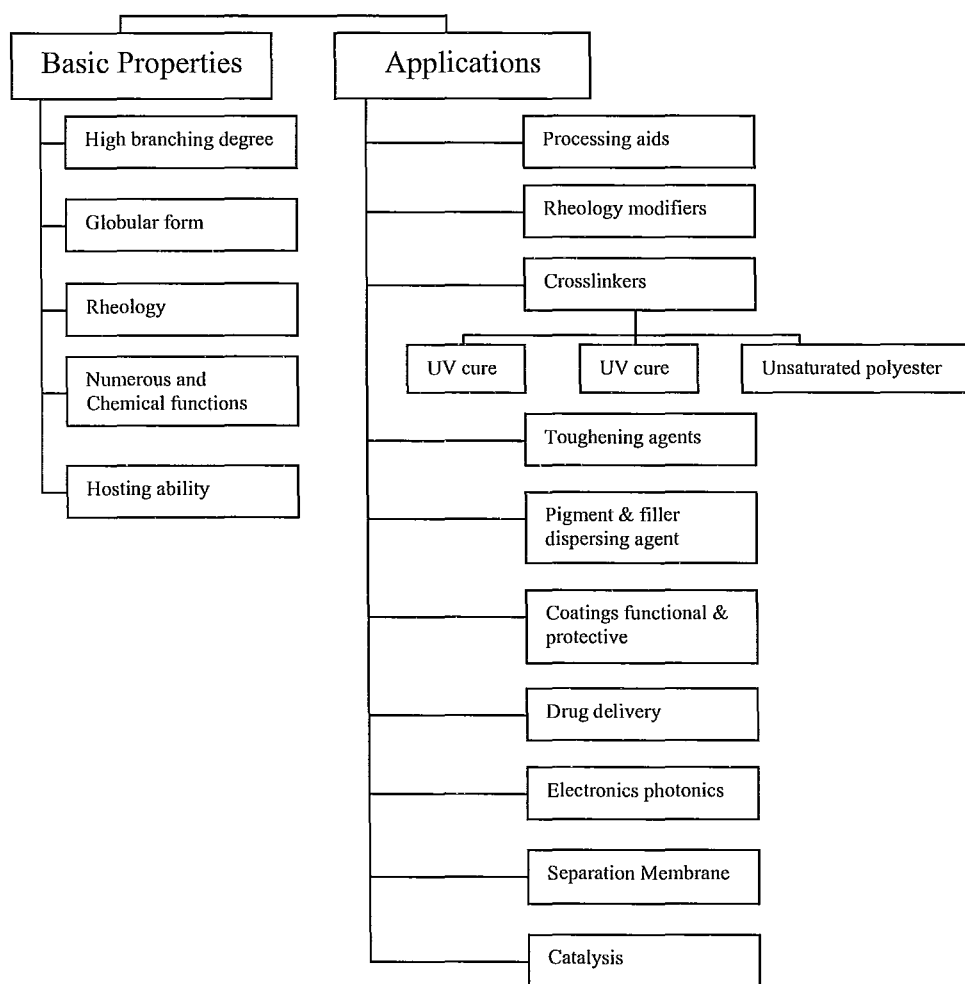


**Figure 1.5:** Properties and application of dendrimers and hyperbranched polymers [12].

### 1.2.2 Hyperbranched Polyethylene Synthesis

Architectural control over resultant polyethylene topology is achieved by coordination polymerization of ethylene with a Pd- $\alpha$ -diimine catalyst (first developed by Brookhart et al. [13]), which undergoes a chain walking mechanism (Figure 1.6).

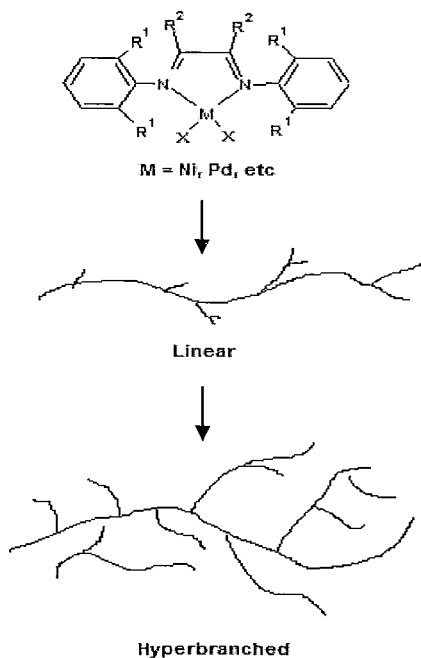


**Figure 1.6:** Schematic for the possibility of formation of linear and hyperbranched polymers from metal based catalysts [14].

The chain walking catalyst introduces the branching (Figure 1.7) by controlling the position of the next monomer addition as it walks on the polymer chain during propagation. Branches are formed as the monomer can add itself to any internal position on the polymer backbone rather than just the chain ends [14, 15].

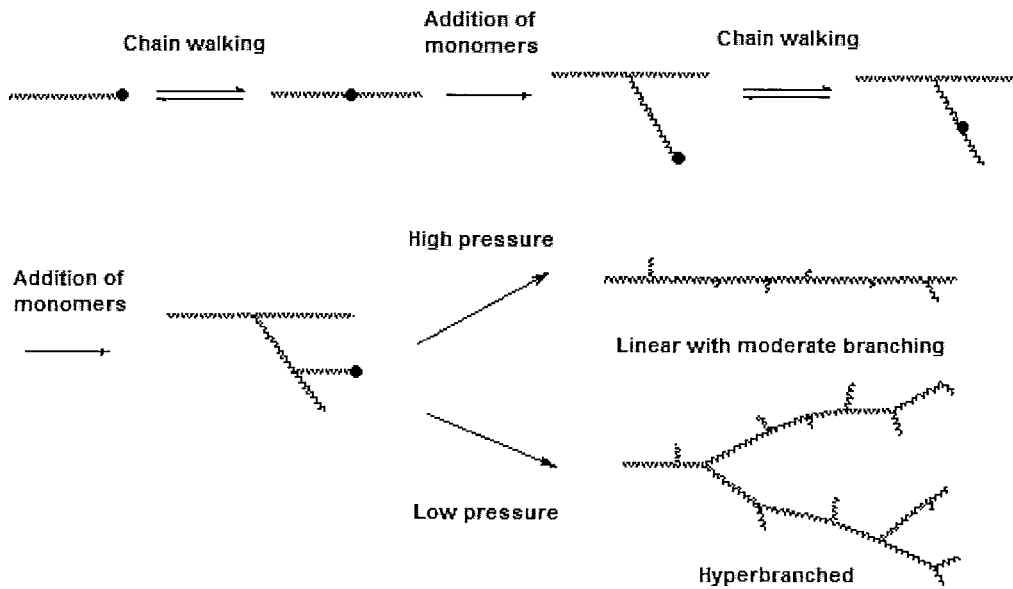


Figure 1.7: Schematic of the chain-walking mechanism [15].

Polyethylenes with various chain topologies can be produced by changing the polymerization conditions which in turn results in controlling the rate of monomer insertion relative to chain walking. For instance, high ethylene pressure and/or low reaction temperatures result in linear polyethylene as the catalyst does not have the capability of walking too far after each insertion. Alternatively, hyperbranched or dendritic polyethylene is produced at low ethylene pressure and/or high temperatures which favor the rate of catalyst walking with respect to the rate of monomer insertion [14, 15].

### 1.3 Polymer Modification

#### 1.3.1 Introduction

Vast amount of research and effort has been applied to develop materials with improved performance and properties on one hand, and to be economically affordable on the other hand. Polymerization and copolymerization of new monomers, blending of existing polymers, and modification of existing polymers are the routes that could be taken to achieve this target, however from an industrial standpoint. The latter routes are more efficient and less costly to pursue [16, 17].

Chemical modification of already existing polymers is typically carried out by chain scission (degradation), crosslinking, and grafting. Those mechanisms are looked at more closely in Chapter 2; with modification by grafting as the major focus of this thesis.

#### 1.3.2 Modification by Grafting

Grafting occurs when a pre-polymer with internal double bonds and/or labile protons is processed together with other saturated or unsaturated compounds [18]. The compound grafted onto the polymer backbone is responsible for the property enhancement [19].

Modification of polyolefins by grafting has received considerable attention in the past few decades [20], using an unsaturated functional monomer, most commonly, maleic anhydride, glycidyl methacrylate, acrylic acid, and diethyle maleate, accompanied with a

peroxide initiator, such as dicumyl peroxide. By far, maleic anhydride functionalized polyolefins are the most important class of polymers, which have found a wide array of commercial applications [21]; they have been extensively used in the compatibilization of immiscible polymer blends as well as the improvement of interfacial adhesion in polymeric composites [22]. In spite the impact of such polymers and their commercial success, the exact chemical mechanism for the functionalization reaction is still vague and unclear.

Functionalization reactions are typically carried out by free radical initiation in melt [23-25], solution [26, 27], and suspension [28]. Other studies used ultrasonic [29], thermomechanical [30] initiation, and photografting [31], to initiate melt functionalization. Reactions performed in solution yield a relatively homogeneous mixture, as the monomer and polymer are usually soluble, and therefore easily mixed. However, reactions conducted in melt are more advantageous from an industrial point of view, as the modification is very fast and there is no need for solvent recovery [32], although they tend to lead to undesirable side reactions, which can damage the processability and properties of the resultant product [33].

Several studies have shown that the reaction pathways depend on the polyolefin molecular structure. In a grafting reaction, where peroxide is used as an initiator, crosslinking and chain scission may occur simultaneously, but with varying dominance, depending on the type of material being grafted; possible reaction routes for

polypropylene and polyethylene are shown in Figures 1.8 and 1.9, respectively. The dominant side reaction for polypropylene is chain scission [34], which occurs because of the initially formed radicals undergoing  $\beta$ -scission, due to the tertiary carbon centers on the polymer backbone (Figure 1.10). On the other hand, the dominant side reaction for polyethylene is crosslinking [35, 36], which occurs due to radical-radical combination (Figure 1.11). In the case of ethylene/propylene rubber, both crosslinking and chain scission can take place, as its properties are a blend of those exhibited by polyethylene and polypropylene [37]. Homopolymerization is another undesirable side reaction that may occur when maleic anhydride is used as the functionalization monomer, which not only decreases the grafting density on the polymer backbone, but also induces coloration of the end-product due to the formation of residual poly(maleic anhydride) [24].

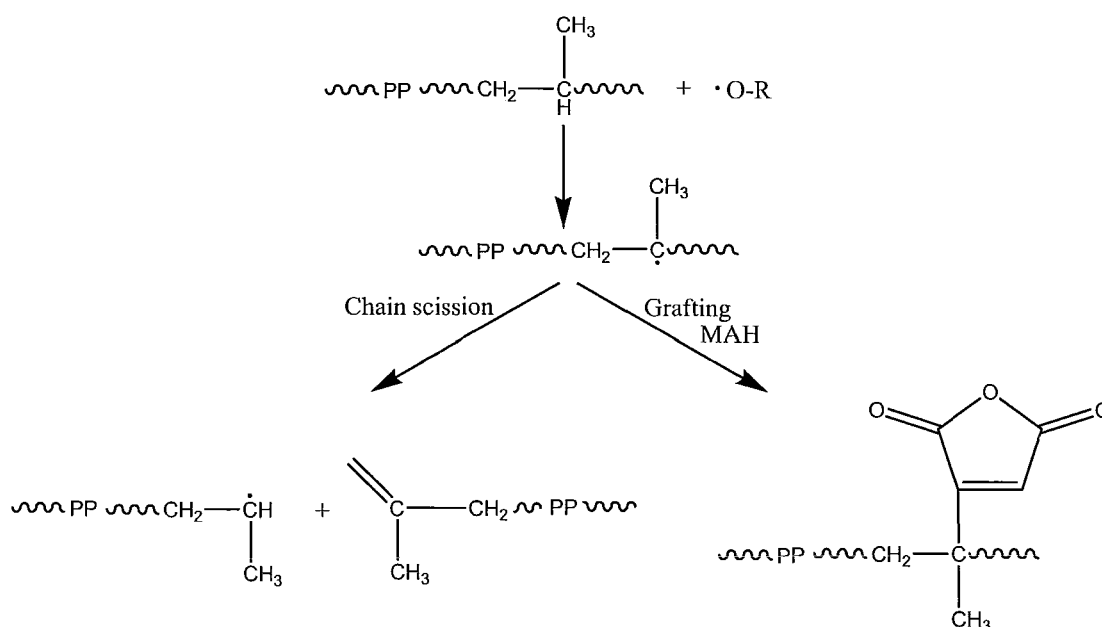


**Figure 1.8:** Possible reaction of the grafting of PP with MAH [38].

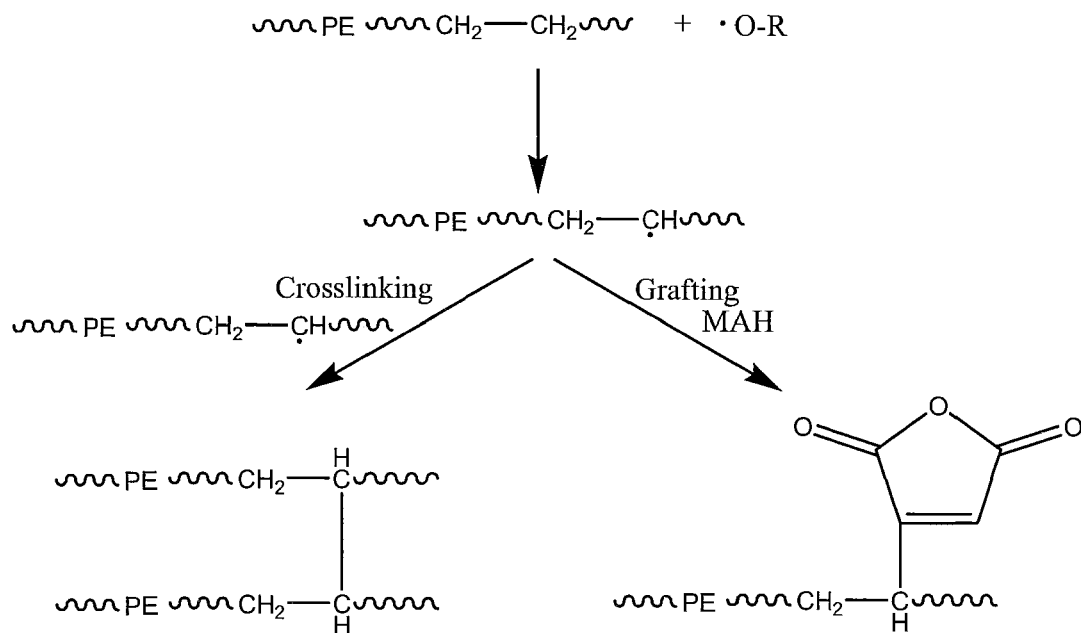


Figure 1.9: Possible reaction of the grafting of PE with MAH [38].

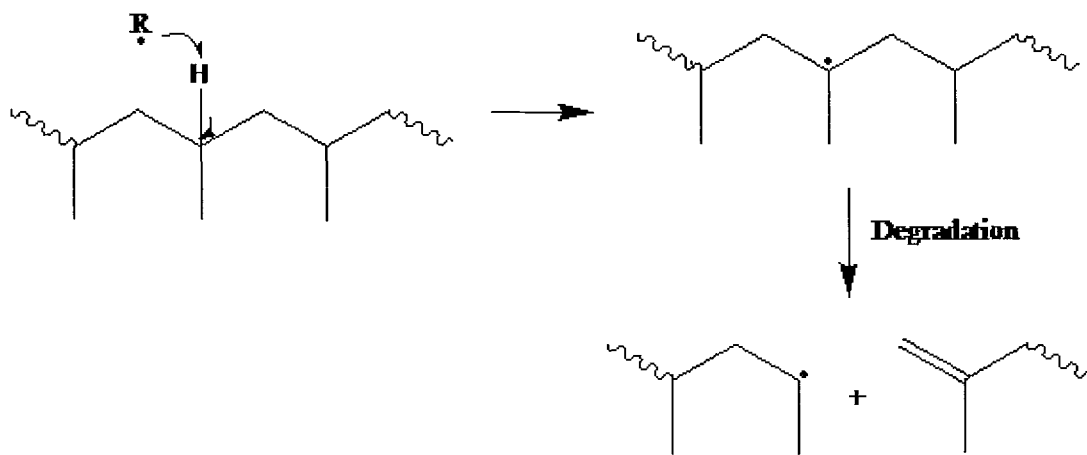
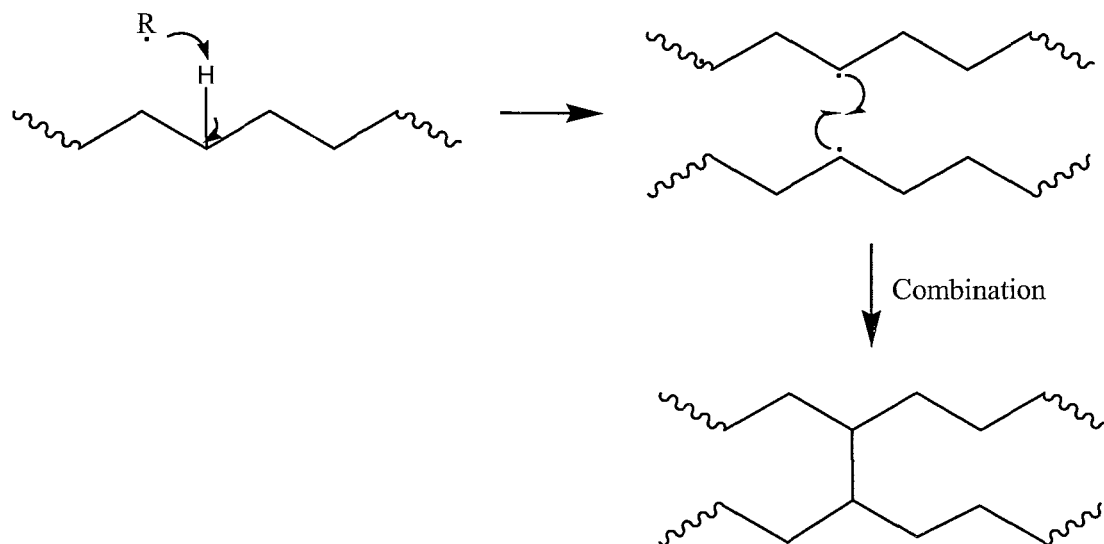


Figure 1.10: Degradation mechanism of polypropylene [38].



**Figure 1.11:** Crosslinking mechanism of polyethylene [38].

### 1.3.3 Effect of Process Conditions

The success of grafting is usually measured in terms of grafting density, which is the fraction of the monomer grafted onto the polymer backbone as opposed to the fraction that was unused or lost to undesirable side reactions such as homopolymerization.

Reaction efficiency, on the other hand, is used to describe the moles of monomer grafted versus the moles of generated initiator derived radicals.

A large number of interdependent variables need to be optimized, in order to maximize grafting density and reaction efficiency, decrease the extent of undesirable side reactions, and control the nature of the grafted product. Those factors are outlined below and summarized in Table 1.1 below [38]:

- I. **Mixing Efficiency** – local reactant concentration is determined by the mixing efficiency, therefore it is crucial to ensure intimate mixing between the monomer, initiator, and the polyolefin.
- II. **Temperature** – polyolefin degradation is often favored by elevated temperatures, which also reduce initiator half-life, modify the rate of reactions, and influence solubility and rheological parameters.
- III. **Pressure** – enhanced solubility, and reduced degradation can be achieved under high-pressure conditions.
- IV. **Monomer** – monomer concentration, solubility, volatility, reactivity towards initiator and substrate derived radicals, susceptibility to homopolymerization need to be considered when choosing a monomer.
- V. **Initiator** – initiator half-life, concentration, volatility, solubility, partition coefficient in polyolefin and monomer, in addition to reactivity and specificity of initiator-derived radicals, are the factors to be considered when choosing an initiator.

**Table 1.1:** Effect of process conditions on side reaction and grafting yields [38].

Condition	To minimize			To maximize
	Crosslinking	Chain scission	Homopolym.	Grafting
Mixing efficiency	Raise	Raise	Raise	Raise
Temperature	Raise	Lower	---	Raise
Pressure	Raise	Lower	Raise	Raise
Monomer concentration	---	Raise	Raise	Raise
Radical concentration	Lower	Lower	Lower	Raise

#### 1.4 Thesis Research Objectives and Outlines

Following the vast developments in the polyolefin field over the past few decades, and the continuous need for the design and synthesis of new specialty polymers that can create a new array of applications, and more doors of research, the overall objectives of this thesis research are to:

- I. Design and synthesize a new hyperbranched polyethylene material by chemical modification, specifically via peroxide-induced maleic anhydride grafting,
- II. Characterize the newly developed polyolefin material, and compare its properties to other major types of polyolefins, and
- III. Establish a potential application for the newly developed material.

In Chapter 2, peroxide-initiated modification of hyperbranched polyethylene and other major types of commercially available polyolefins was conducted to determine the standpoint of hyperbranched polyethylene to other polyolefins in terms of degradation/crosslinking.  $^{13}\text{C}$ -NMR and DEPT-135 NMR were used to quantify the number of CH, CH<sub>2</sub>, and CH<sub>3</sub> groups before and after modification, while creep-recovery rheological measurements were used to evaluate the zero shear viscosity of the materials before and after their modification.

In Chapter 3, functionalization of hyperbranched polyethylene with maleic anhydride was conducted by peroxide initiation, where the effect of various process conditions and parameters on the grafting density and reaction efficiency was investigated. Quantification of grafting density was performed through titrations, while FTIR and high temperature  $^1\text{H-NMR}$  were used to confirm grafting. Water contact angle measurements were used to investigate the effect of grafting on the water contact angle and hence the properties of the resultant polymer.

In Chapter 4, rheological characterization of hyperbranched polyethylene, and hyperbranched polyethylene grafted with maleic anhydride was conducted for comparison reasons. Steady shear, oscillatory, and creep recovery measurements were conducted to compare the rheological properties and the viscosities of the grafted polymer and the ungrafted counterpart, and to investigate whether the grafted polymer maintained the Newtonian behavior exhibited by its parent polymer upon grafting.

In Chapter 5, crosslinking of hyperbranched polyethylene grafted with maleic anhydride was conducted by the use of a diamine as a crosslinking agent. The effect of multiple process parameters on the degree of crosslinking (gelation) was examined, where the degree of crosslinking was measured by a Soxhlet apparatus, and crosslinking was confirmed by FTIR. Nonetheless, examination of whether this process could yield a potential material for reaction injection molding was also performed.

## 1.5 References

- [1] Nexant, Inc. (2008). *Olefins and Polyolefins Cost Competitiveness*. Retrieved April 16, 2008, from [http://www.chemsystems.com/about/cs/news/items/POPS07\\_SUPP\\_III.cfm](http://www.chemsystems.com/about/cs/news/items/POPS07_SUPP_III.cfm)
- [2] Nexant, Inc. (2008). *New Industry Outlooks for Polyethylene and Polypropylene*. Retrieved April 16, 2008, from <http://www.chemsystems.com/about/cs/news/items/New%20Industry%20Outlooks%20for%20Polyethylene%20and%20Polypropylene.cfm>
- [3] IAL Consultants. *Advanced Polyolefins - The competitive Position*. London: IAL Consultants, 2000
- [4] Seymour, R.; Cheng, T. *Advances in Polyolefins – The World’s Most Widely Used Polymers*, Plenum Press, 1987, pg. 9
- [5] Creative Commons Attribution. (2008). *Introduction to Polymers*. Retrieved April 8, 2008, from <http://openlearn.open.ac.uk/mod/resource/view.php?id=196631>
- [6] Peacock, A. *Handbook of Polyethylene: Structures, Properties, and Applications*, CRC Press, 2000
- [7] Fischer, M.; Vogtle, F. *Angew. Chem. Int. Ed.* 1999, 38, 884
- [8] Hult, A.; Johansson, M.; Malmstrom, E. *Adv. Polym. Sci.* 1999, 143, 1
- [9] Brunsveld, L.; Folmer, B.; Meijer, E.; Sijbesma, R. *Chem. Rev.* 2001, 101, 4071
- [10] A. Hult, M. Johansson, E. Malmstrom, *Adv. Polym. Sci.* 1999, 143, 1
- [11] Kim, Y.; Webster, O. *Macromolecules.* 1992, 25, 5561

- [12] SpecialChem S.A. (2008). *The breakthrough of dendrimers and hyperbranched polymers*. Retrieved April 7, 2008, from <http://www.specialchem4polymers.com/resources/articles/article.aspx?id=2696>
- [13] Johnson, L.; Killian, C.; Brookhart, M. *J. Am. Chem. Soc.* **1995**, 117, 6414
- [14] Z. Guan. *Chem. Eur. J.* **2002**, 8, 3087
- [15] Z. Guan, P.M. Cotts, E.F. McCord, S.J. McLain, *Science* **1999**, 283, 2059
- [16] Xanthos, M. *Reactive Extrusion*. New York: Hanser, **1992**
- [17] Al-Malaika, S. *Reactive Modifiers for Polymers*. London: Blackie Academic and Professional, **1997**
- [18] Machado, A.; Covas, J.; van Duin, M. *Polymer* **2001**, 42, 3649
- [19] Hamielec, A.; Gloor, P.; Zhu, S. *Canadian Journal of Chem. Eng.* **1991**, 69, 611
- [20] Ho, R.; Su, A.; Wu, C. *Polymer*. **1993**, 34, 3264
- [21] Sheshkali, H.; Assempour, H.; Hazockdast, H. *J. App. Polym. Sci.* **2007**, 105, 1869
- [22] Gaylord, N. *Chemtech*, **1989**, 19, 435
- [23] Gaylord, N.; Mehta, R.; Kumar V.; Tazi, M. *J. App. Polym. Sci.* **1989**, 38, 359
- [24] Gaylord, N.; Mehta, R.; Mohan, D.; Kumar, V. *J. App. Polym. Sci.* **1992**, 44, 1941
- [25] Aghjeh, M.; Nazokdast, H.; Assempour, H. *J. App. Polym. Sci.* **2006**, 99, 141
- [26] Liu, N.; Baker, W.; Russell, K. *J. Appl. Polym. Sci.* **1990**, 41, 2285
- [27] Wang, Y.; Ji, D.; Yang, C.; Zhang, H.; Qin, C.; Huang, B. *J. App. Polym. Sci.* **1994**, 52, 1411
- [28] Lu, B.; Chung, T. J. *Polym. Sci. Part A: Polym. Chem.* **2000**, 38, 1337
- [29] Zhang, Y.; Li, H. *Polym. Eng. Sci.* **2003**, 43, 774

- [30] Lusinchi, J.; Boutevin, B.; Torres, N.; Robin, J. *J. app. Polym. Sci.* **2001**, 79, 874
- [31] Jianping, D.; Wantai, Y. *J. App. Polym. Sci.* **2003**, 87, 2318
- [32] Machado, A.; Covas, J.; van Duin, M. *Polymer* **2001**, 42, 3649
- [33] Sheshkali, H.; Assempour, H.; Nazockdast, H. *J. App. Polym. Sci.* **2007**, 105, 1869
- [34] Gaylord, N.; Mehta, M.; Mehta R. *J. App. Polym. Sci.* **1987**, 33, 2549
- [35] Greco, R.; Musto, P.; Riva, F.; Maglio, G. *J. App. Polym. Sci.* **1989**, 37, 789
- [36] Rosales, C.; Perera, R.; Ichazo, M.; Gonzalez, J.; Rojas, H.; Sanchez, A.; Barrios, A. *J. App. Polym. Sci.* **1998**, 70, 161
- [37] Garcia-Martinez, J.; Laguna, O.; Collar, E. *J. Appl. Polym. Sci.* **1998**, 68, 483
- [38] Moad, G. *Prog. Polym. Sci.* **1999**, 24, 81

## **Chapter 2: Peroxide Modification of Polyolefins**

### 2.1 Introduction

#### 2.1.1 Polymer Chemical Modification

Polymer industry has grown exponentially in the past few decades, where polymers started playing a vital role in all aspects of human life. Most of the widely used polymers are categorized as commodity polymers. Commodity polymers are large volume consumption polymeric materials, which are typically sold for less than \$1/kg. The properties of such polymers and their processability limit their use to general-purpose applications. Such polymers include high-density polyethylene (HDPE), low-density polyethylene (LDPE), linear low-density polyethylene (LLDPE), polypropylene (PP), polystyrene (PS), polyvinyl chloride (PVC), and polyacrylics. Commodity polymers can generally be upgraded to specialty polymers via chemical modification, where specialty polymers are those polymers, which are strictly needed for special uses and specific applications, and they tend to be very expensive (> \$1/kg).

Chemical modification of polymers generally occurs via chain scission or degradation, long chain branching, crosslinking, and grafting. The commercial incentive for chemical modification is to economically enhance physical and chemical properties of polymers and polymer mixtures and/or improve their processability [1]. Thorough explanation of chemical modification reactions follows.

### ***Chain Scission or Degradation***

Polymer chain scission occurs when chemical bonds (usually C-C bonds) along the polymer backbone break. Higher molecular weight chains undergo random chain scission preferentially since they have a greater number of bonds, therefore for broad molecular weight distributions, the breadth of the molecular weight distribution narrows, becoming more random (Flory's most probable distribution), as the mean molecular weight decreases. Improved processability due to a reduction in melt viscosity is a result of chain scission, which primarily leads to a reduction in molecular weight.

### ***Long Chain Branching and Crosslinking***

Long chain branches are formed when radical centers on polymer backbones undergo bimolecular termination by combination. Continuation of the long chain branching process could result in a three dimensional network with different levels of crosslinked gel.

Crosslinking of polymer chains results from repetitive bimolecular coupling of polymer chains via bimolecular termination of radical centers on polymer backbones. The crosslinked polymer is a mixture of crosslinked gel with infinite molecular weight (in theory), and sol, which is made up of linear and branched chains.

### ***Grafting***

Grafting occurs when a pre-polymer with internal double bonds and/or abstractable protons is processed together with other saturated or unsaturated compounds

[2]. The compound grafted onto the polymer backbone is responsible for the property enhancement [1].

### 2.1.2 Peroxides for Chemical Modification

Organic peroxides are a large group of molecules, which contain a relatively thermally unstable O-O bond. This bond is susceptible to break once heat is applied, forming aggressive free radicals. Those free radicals are capable of abstracting hydrogen atoms from a polymer backbone forming macroradicals, which can undergo any of the previously mentioned reactions: grafting, chain scission, crosslinking, and long chain branching. The decomposition mechanism of commonly used peroxide, namely, dicumyl peroxide is shown in Figure 2.1. Decomposition of an initiator molecule is a monomolecular reaction, so the decomposition rate is solely dependent on reaction temperature, while the initiator concentration has no effect on the decomposition rate [3].

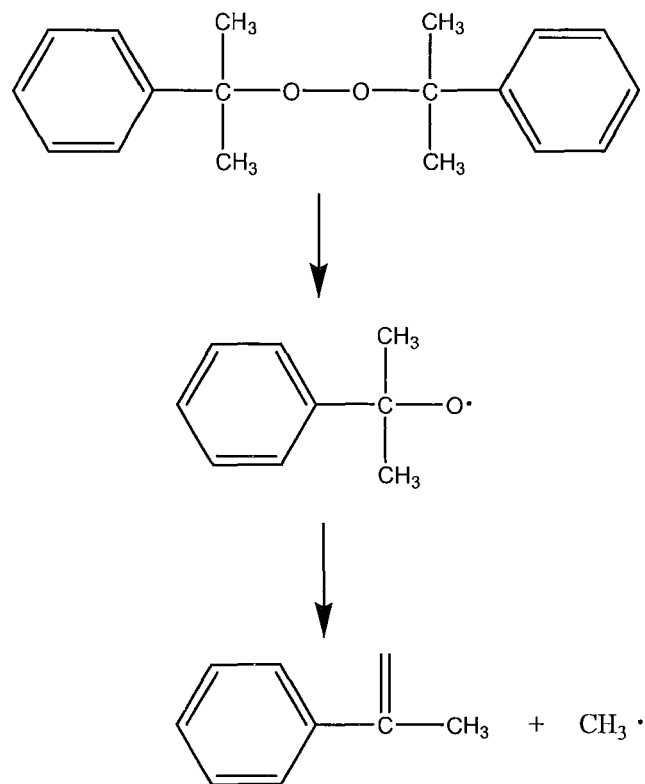


**Figure 2.1:** Dicumyl peroxide decomposition mechanism.

The choice of organic peroxides for the modification of polyolefins is dependent on the properties of the peroxide itself, which include processing temperature, cure temperature, and crosslinking efficiency. Table 2.1 presents a summary of these properties for the two initiators worked with throughout this thesis, namely, dicumyl peroxide and dibenzoyl peroxide.

**Table 2.1:** Survey of commercial peroxides [3].

	Safe processing temperature (°C)	Typical cure temperature (°C)	Crosslinking efficiency $\epsilon$ (%)*
<b>Dicumyl peroxide</b>	120	170	50
<b>Dibenzoyl peroxide</b>	70	120	27
*As determined in n-pentadecane			

### 2.1.3 $^{13}\text{C}$ -NMR Characterization

$^{13}\text{C}$ -NMR is used extensively in the characterization of molecules, as many of the molecules that exist in nature contain carbon.  $^{13}\text{C}$  nucleus has a nuclear spin due to the unpaired electron present in its orbit.  $^{13}\text{C}$ -NMR is much less sensitive than  $^1\text{H}$ -NMR, because  $^{13}\text{C}$  nuclei make up approximately 1% of overall carbon nuclei available in nature. With the appropriate conditions, carbon-13 NMR spectroscopy can be used to supplement the information obtained from  $^1\text{H}$ -NMR [4].

Conducting quantitative analysis on  $^{13}\text{C}$ -NMR can be very challenging due to two well recognized problems. Firstly, the long relaxation times for different types of carbon nuclei results in the need for long pulse delays to ensure that all nuclei are relaxed and in their equilibrium state before the application of any repetitive pulse. Secondly, more intense signals are generated for carbon nuclei that tend to be highly protonated, and this is known as the unequal Nuclear Overhauser Enhancement (NOE). Thus, both problems can be circumvented by applying a long pulse delay, and by adjusting other instrumental parameters; however this is unfavorable as it increases spectrum recording time.

To shorten the relaxation time and hence the spectrum recording time, and at the same time suppress the NOE effects, well-chosen paramagnetic agents that assist in nuclei relaxation are typically added. The most common agents used are acetylacetonates chromium (III) and iron (III) [5].

#### 2.1.4 DEPT<sub>135</sub> Characterization

Distortionless Enhancement by Polarization Transfer (DEPT) is a polarization transfer technique, which is run alongside a <sup>13</sup>C-NMR to distinguish between methyl (CH<sub>3</sub>), methylene (CH<sub>2</sub>), and methane (CH) signals.

The pulse angle ( $\theta$ ) allows for the differentiation between those signals, and creates three different sets of experiments which are typically conducted: DEPT-45, DEPT-90, and DEPT-135, respectively. The angle is set to 45° in the sequence DEPT-45, which yields spectra with positive CH, CH<sub>2</sub> and CH<sub>3</sub> signals; to 90° in DEPT-90, which yields spectra with only CH signals; and to 135° in DEPT-135, which yields spectra with positive CH and CH<sub>3</sub> signals and negative CH<sub>2</sub> signals [6]. Figure 2.2 is an illustration of correlating DEPT spectra to a <sup>13</sup>C spectrum.

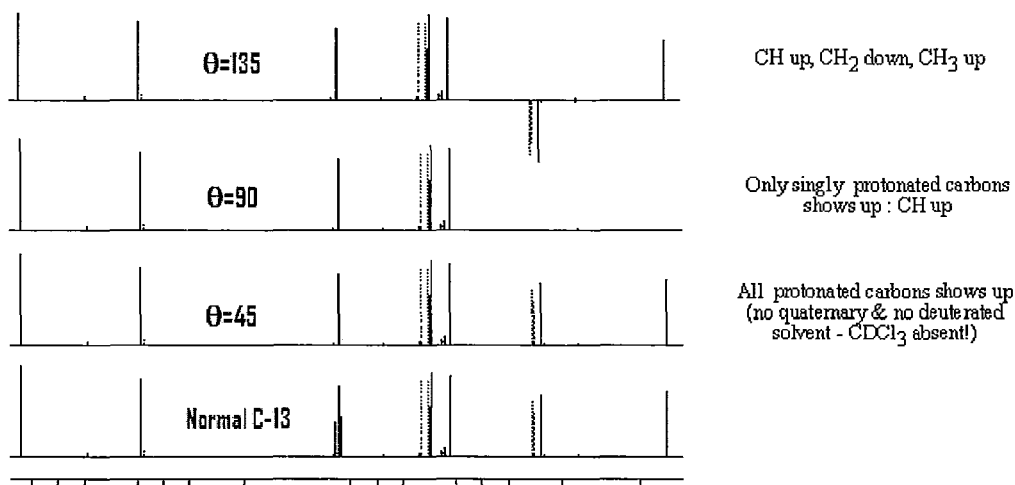


**Figure 2.2:** Illustration of correlating DEPT spectra to a  $^{13}\text{C}$  spectrum [7].

### 2.1.5 Determination of Zero Shear Viscosity from Creep-Recovery Experiments

Materials which are defined as elastic, viscous, or viscoelastic exhibit different responses in a creep-recovery experiment (Figure 2.3); where a sudden stress is applied to the samples and the resultant strain is measured. Viscoelastic materials undergo a superposition of both the elastic and viscous responses [8].

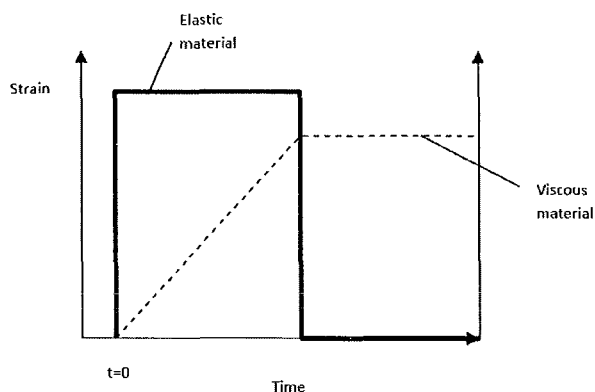


**Figure 2.3:** Illustration of creep-recovery results characteristic of elastic and viscous materials, respectively [8].

Creep recovery measurements facilitate the separation of the total deformation to its elastic and viscous components, and can also give information about the zero shear viscosity of a material.

Zero shear rate viscosity ( $\eta_0$ ) is defined as the lower end limit of viscosity measured with respect to shear rate [9]. It is an important rheological parameters used in the polymer industry, and its value is typically determined at the end of the creep phase.

When conducting a creep-recovery test, the aim should be to produce a creep curve with a constant slope at the end of the creep curve, where the zero shear viscosity is obtained from this curve interval as shown in Figure 2.4. First, slope of the strain-time curve is calculated ( $\Delta\gamma/\Delta t$ ). Second, zero shear viscosity is calculated from stress applied divided by the slope of the strain-time curve (Figure 2.4) [10].

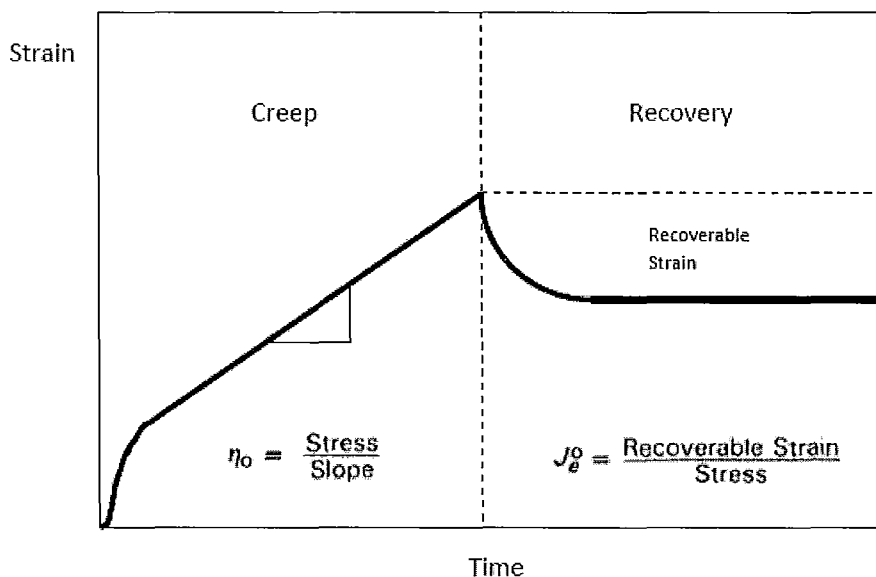


**Figure 2.4:** Strain vs. time curve obtained from creep-recovery experiment is shown. The slope of the creep curve is used in conjunction with the stress applied to calculate the respective shear rate viscosity [11].

### 2.1.6 Objective and Scope

The target of this chapter is to examine the behavior of hyperbranched polyethylene relative to other commercially available polyolefins in terms of whether it will undergo degradation or crosslinking upon peroxide-initiated modification.

Different grades of commercially available polyolefins and hyperbranched polyethylene were modified by peroxide initiation.  $^{13}\text{C}$ -NMR and rheology techniques were used to investigate the effect of modification on their respective structures.  $^{13}\text{C}$ -NMR was used to find the  $\text{CH}$ ,  $\text{CH}_2$ , and  $\text{CH}_3$  content in the polymer before and after modification, while creep-recovery was used to evaluate the percentage change in viscosity of the modified material relative to the starting material.

## 2.2 Experimental

### 2.2.1 Materials

Hyperbranched polyethylene (HBPE) with a molecular weight of 100,000 g/mol was kindly supplied by Dr. Zhibin Ye's Group – University of Laurentian, Ontario, Canada. Moreover, high density polyethylene (HDPE-F00952), low density polyethylene (LDPE-HP0322N), and linear low density polyethylene (LLDPE-118) were supplied by Sabic, Saudi Arabia, while polypropylene (PP) was supplied by British Petroleum. Furthermore, dicumyl peroxide (DCP) - 98 % purity, was purchased from Aldrich. Finally, xylenes solvent was purchased from Fisher Scientific.

### 2.2.2 Peroxide Modification of Polyolefin

Prior to addition of initiator, 2 g of a polyolefin, namely, PP, LDPE, LLDPE, HDPE, and HBPE, was added to a 200 mL xylene solution at 130 °C, and was allowed to homogenize for 1 hr. After 1 hr, 10 wt.% DCP was added to the solution, and reaction was left for 5 hrs running at 130 °C under a nitrogen blanket. Upon completion of the reaction, modified polymer was precipitated using 5-fold volume of acetone. Finally, modified polymer was filtered and dried under vacuum at 115 °C over night.

### 2.2.3 <sup>13</sup>C-NMR and DEPT<sub>135</sub> Sample Preparation

To a NMR tube, polyolefin (0.1 g) and 1,1,2,2-tetrachloroethane-d<sub>4</sub> were added and heated at 120 °C for 1 hr, to achieve homogenization. Subsequently, 80 mg of Cr(acac)<sub>3</sub> was added to the NMR tube, and the mixture was further heated for 30 minutes.

Finally, the NMR tube was inserted into the NMR machine for analysis.  $^{13}\text{C}$ -NMR and DEPT\_135 experiments were conducted at 120 °C using a 30° pulse angle of 6  $\mu\text{s}$ , an acquisition time of 1 s, a preparation delay time of 2 s, and 12,000 scans. For the  $^{13}\text{C}$ -NMR experiment, inverse gated decoupling was used to eliminate NOE effects. All measurements were repeated twice to confirm reproducibility.

#### 2.2.4 Disk Preparation

Using a thermal press, thick disks of polyolefins for rheological characterization were prepared with the following dimensions: 25 mm diameter, and 1 mm thickness. Disks were compression molded for 3 mins at a temperature, which is 20 to 30 °C greater than the melting temperature of the used polyolefin.

#### 2.2.5 Rheological Characterization

Rheological characterizations were conducted on a Stresstech HR rheometer; in a 25 mm parallel plate mode with a gap of 1.0 mm. Measurements were taken at 10 °C intervals at temperatures, which are 10 to 20 °C above the melting point of the tested polyolefin. The temperature of the rheometer was maintained within  $\pm 0.2$  °C. Polymer samples were subject to creep recovery. In the creep recovery experiments, samples were subject to a stress at time zero, and the compliance was monitored at constant stress for 100 s, then the stress was removed, and the relaxation behavior was recorded. All measurements were conducted on the same loaded sample [12], and repeated twice to confirm reproducibility.

## 2.3 Results and Discussion

### 2.3.1 $^{13}\text{C}$ -NMR Characterization of As Received and Modified Polyolefins

$^{13}\text{C}$ -NMR and DEPT\_135 NMR were used in situ to quantify the number of CH, CH<sub>2</sub>, and CH<sub>3</sub> groups for as received hyperbranched polyethylene, other commercially available polyolefins, and their peroxide-initiated counterparts. The results are tabulated in Table 2.2. PP, HDPE, LDPE, LLDPE, and HBPE were used in this study.

**Table 2.2:** Number of CH, CH<sub>2</sub>, CH<sub>3</sub>, and vinylidene groups for unmodified and modified polyolefins. Results obtained by integrating the peaks in the  $^{13}\text{C}$ -NMR spectra. Spectra obtained using a 30° pulse angle of 6 μs, an acquisition time of 1s, a preparation delay time of 2s, and 12,000 scans. Spectra recorded at 120 °C using 1,1,2,2-tetrachloroethane-d<sub>4</sub> as a solvent, and Cr(acac)<sub>3</sub> as a relaxation agent.

Material	CH	CH <sub>2</sub>	CH <sub>3</sub>	Vinylidene
PP	341	311	309	38
Modified PP	336	308	299	56

Material	CH	CH <sub>2</sub>	CH <sub>3</sub>	Vinylidene
HDPE	0	947	0	53
Modified HDPE	0	947	0	53

Material	CH	CH <sub>2</sub>	CH <sub>3</sub>	Vinylidene
LDPE	8	971	10	11
Modified LDPE	0	989	11	0

Material	CH	CH <sub>2</sub>	CH <sub>3</sub>	Vinylidene
LLDPE	16	969	15	0
Modified LLDPE	15	968	17	0

Material	CH	CH <sub>2</sub>	CH <sub>3</sub>	Vinylidene
HBPE	84	823	87	6
Modified HBPE	70	827	98	5

DEPT\_135 with a  $135^\circ$  decoupler pulse was used to distinguish the CH, CH<sub>2</sub>, and CH<sub>3</sub> peaks. This pulse sequence produces a carbon spectrum where methyl (CH<sub>3</sub>) and methyne (CH) carbons are up, while methene (CH<sub>2</sub>) carbons are down.

A  $^{13}\text{C}$ -NMR spectrum free of coupled carbons and NOE (Nuclear Overhauser Effect) was achieved by using the Inverse gated decoupling method [13]. A relaxation agent Cr(acac)<sub>3</sub> was also added to expedite the relaxation of the different carbon nuclei and hence shorten the spectra recording time.

Analysis of the results obtained for the different types of polyolefins (Table 2.2) is as follows:

### *Polypropylene*

Polypropylene typically undergoes degradation through  $\beta$ -scission (Figure 2.5), which results in the formation of vinylidene groups, along with the consumption of CH groups.

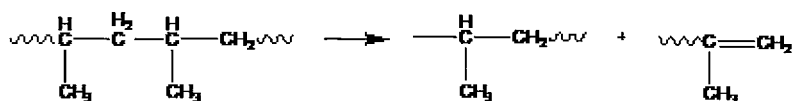


**Figure 2.5:** Chain scission in PP [14].

The decrease in the number of CH and CH<sub>3</sub> groups, in addition to the significant increase in the vinylidene content, suggests that PP underwent a degradation reaction. Degradation is the most common reported reaction for peroxide-initiated modification of PP. PP has a high degree of branching, and degradation primarily occurs due to the methyne carbon, which is susceptible to undergo  $\beta$ -scission.

### *High Density Polyethylene*

HDPE generally undergoes crosslinking by bimolecular recombination of backbone radicals (Figure 2.6) [15], which generally involves consumption of protons due to the formation of radicals on the polymer backbone, accompanied by a decline in the number of CH<sub>2</sub> groups, and the formation of CH groups. HDPE used in this study was synthesized using a Z-N catalyst system forming a polymer majorly composed of very long chains with very low solubility in the solvent used. Only the tiny fraction of short chains was soluble in the solvent, which led to the detection of the vinylidene end groups of those short chains and no CH<sub>3</sub> groups. No evidence of crosslinking or degradation was detected for these soluble fractions from <sup>13</sup>C-NMR showing only a linear chain. Any changes in the molecular composition of the polymer upon crosslinking were not detectable. The CH<sub>2</sub> and vinylidene contents of the as-received form and the modified form remained constant, while no CH and CH<sub>3</sub> groups were observed.

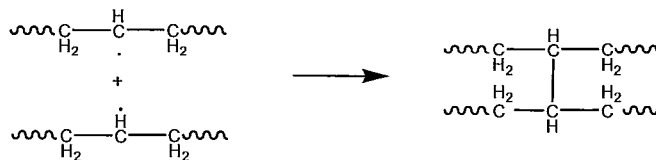


**Figure 2.6:** Bimolecular recombination of backbone radicals in HDPE [15].

### *Low Density Polyethylene*

Upon hydrogen abstraction from the LDPE backbone, the following alkyl radicals are formed (Figure 2.7), which are mainly secondary and tertiary carbon radicals, including allylic carbon radicals. This stage involves the consumption of protons, and hence CH and CH<sub>2</sub> groups.

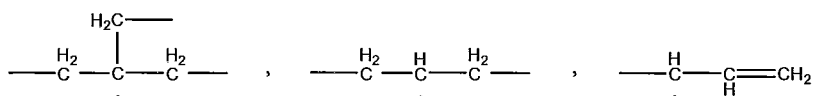


**Figure 2.7:** Radicals formed upon hydrogen abstraction from LDPE backbone [16].

When the above radicals undergo recombination with each other, structures in Figure 2.8 are formed, which involve the formation of CH groups.

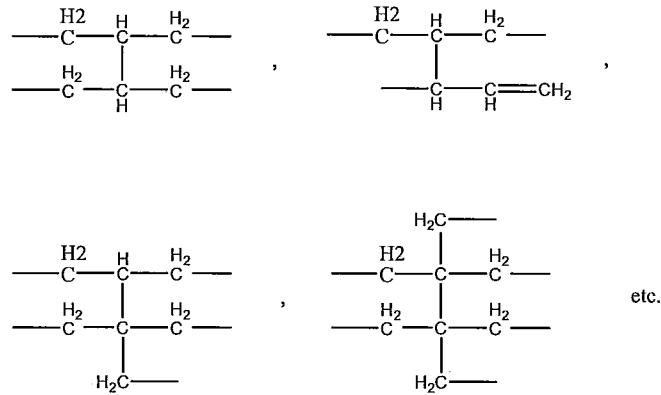


**Figure 2.8:** Structures formed due to the recombination of radicals in LDPE [16].

Nonetheless, addition of radicals in Figure 2.7 to vinyl groups results in the formation of the following structures (Figure 2.9). This stage involves formation of  $\text{CH}_2$  groups, and consumption of vinylidene groups.

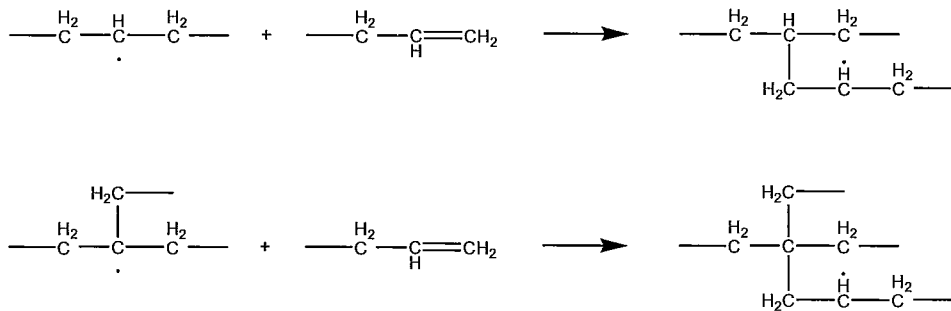


**Figure 2.9:** Radical addition to vinyl groups in LDPE [16].

The significant decrease in the vinylidene content and the increase in the number of  $\text{CH}_2$  groups upon modification conclude that LDPE mainly underwent crosslinking, which suggests that most of the crosslinking occurred due to radical addition to the vinyl groups in LDPE, rather than radical-radical combination. The number of  $\text{CH}_3$  branches

remained constant, while the number of CH groups decreased upon modification, which demonstrates that some degradation also took place.

### ***Linear Low Density Polyethylene***

For LLDPE, there was hardly any change in the number of CH, CH<sub>2</sub>, CH<sub>3</sub>, and vinylidene groups. This suggested that there was no reaction among the soluble fraction detected by NMR.

Degradation is expected to occur in LLDPE following the same mechanism as that for PP (Figure 2.5), and crosslinking follows the same route followed by LDPE (Figures 2.8 and 2.9).

### ***Hyperbranched Polyethylene***

A decrease in the number of CH groups, as well as an increase in the number of CH<sub>3</sub> groups upon modification, suggests a degradation reaction. HBPE was susceptible to both crosslinking and degradation as it contains a high degree of branching but also some linear chains; however, degradation seems to be the dominant reaction.

The number of vinylidene groups hardly changed after modification, although an increase in vinylidene content is typical of degradation reaction; the change in the number of vinylidene groups may have been undetectable due to the low content of vinylidene groups compared to the other groups within the polymer molecules. Degradation in HBPE follows the same route as that for PP shown in Figure 2.5, while crosslinking

follows the same mechanism as that for LDPE displayed in Figures 2.8 and 2.9, respectively.

### 2.3.2 Correlation Between Polymer Modification and Zero Shear Viscosity

Zero shear viscosity ( $\eta_0$ ) was calculated from creep-recovery curves as discussed in section 2.1.5. Creep recovery experiments for the polyolefins used in this study were conducted at different ranges of temperatures, because the polyolefins used have different melting temperatures. To eliminate the effect of temperature on this study, the percentage change in zero shear viscosity between the as received and modified polyolefin was calculated at each tested temperature. The percentage changes in  $\eta_0$  for each polyolefin, which were almost identical, were averaged, and results are shown in the bar chart in Figure 2.10. A positive percentage change in  $\eta_0$  indicates an increase in the  $\eta_0$  of the modified polyolefin, which was generally thought to be due to crosslinking. On the other hand, a negative percentage change in  $\eta_0$  indicated a decrease in the  $\eta_0$  of the modified product, and hence degradation of the parent polymer.

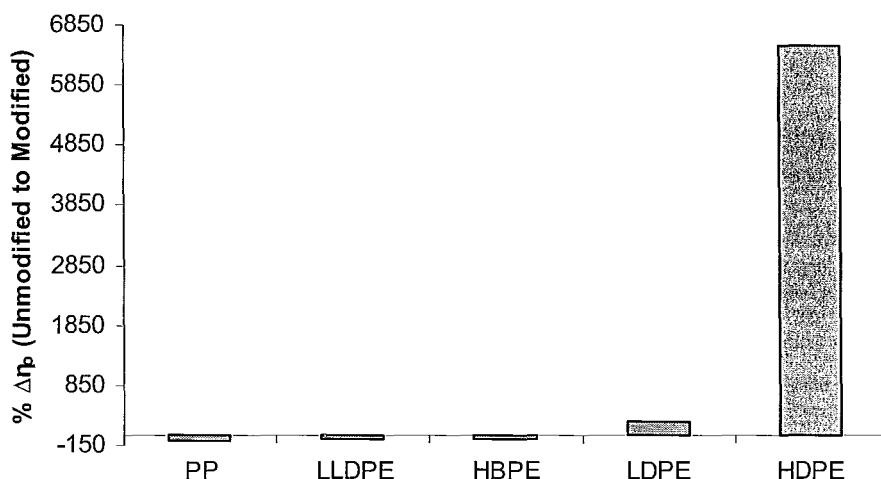


**Figure 2.10:** Percentage change in zero shear viscosity for various polyolefin grades before and after modification. Rheological characterization was conducted 10-20 °C above the melting temperature of each polyolefin, and experiments were conducted at 10 °C intervals. Negative changes in viscosity identify degradation as opposed to crosslinking, which is characterized by positive changes.

From Figure 2.10, it is noticeable that PP, LLDPE, and HBPE underwent degradation, while LDPE and HDPE underwent crosslinking. The high degree of branching in PP creates more methyne carbons on the polymer backbone, which are vulnerable to undergo degradation by  $\beta$ -scission; this agrees with  $^{13}\text{C}$ -NMR results. Since LLDPE and HBPE contain linear chains as well as a certain degree of branching, it is noticeable that degradation was the dominant reaction, which resulted in a decrease in both their zero shear rate viscosities. On the contrary, LDPE, although has both linear chains and some branching, the dominant reaction it underwent upon modification is crosslinking, which resulted in an increase in its zero shear viscosity. A significant increase in zero shear viscosity is evident for HDPE, which is linear in nature.

From the rheological study, it is found that HBPE undergoes degradation as opposed to crosslinking, as it contains branch centers, which are susceptible to  $\beta$ -scission. Some crosslinking also exists due to the linear chains found in HBPE; however, this is not the dominant reaction, as suggested by the decrease in zero shear viscosity upon modification. This concludes that HBPE behaves more like PP in the spectrum of polyolefins, rather than HDPE, which undergoes crosslinking.

## 2.4 Conclusion

This work elucidated that degradation by  $\beta$ -scission is the dominant reaction for peroxide-initiated HBPE modification. Conclusion was made based on results from two characterization techniques, namely,  $^{13}\text{C}$ -NMR and creep-recovery.  $^{13}\text{C}$ -NMR showed that the material before modification has a large content of CH and  $\text{CH}_3$  groups relative to other polyolefins, suggesting that it has a high degree of branching, and therefore susceptible to degradation. Comparison of the number of these groups before and after modification shows that modification was accompanied by a decrease in the number of CH groups, which confirms degradation of the polymer. This hypothesis was further confirmed from zero shear viscosity results obtained from creep-recovery experiments, where a decrease in zero shear viscosity was noticed upon modification, which is a resultant effect of degradation.

Hyperbranched polyethylene was found to behave similar to polypropylene, where they both undergo degradation, as opposed to high-density polyethylene, which

undergoes crosslinking. Herein, the behavior of hyperbranched polyethylene in terms of other commercially available polyolefins was revealed.

## 2.5 References

- [1] Hamielec, A.; Gloor, P.; Zhu, S. *Canadian Journal of Chem. Eng.* **1991**, 69, 611
- [2] Machado, A.; Covas, J.; van Duin, M. *Polymer* **2001**, 42, 3649
- [3] van Drumpt, J. *Rubber World*, **1988**, 33
- [4] Hornak, J. (2006). *Carbon-13 NMR - The Basics of NMR*. Retrieved April 2, 2008, from <http://www.cis.rit.edu/htbooks/nmr/inside.htm>
- [5] Prasad, J.; Rao, P.; Garg, V. *Eur. Poly. J.* **1991**, 27, 251
- [6] BRUKER. *AVANCE User's Guide: DEPT*. Ch.6, pg 66.
- [7] Sauriol, F. (1999). *Multiplet Detection in Coupled or Decoupled <sup>13</sup>C DEPT*. NMR Course Content: Retrieved March 30, 2008, from <http://www.chem.queensu.ca/FACILITIES/NMR/nmr/webcourse/>
- [8] ATS Rheologica. *StressTech Rheometer User's Guide*. Pg 115
- [9] Hackley, V.; Chiara, F. *NIST: Guide to Rheological Nomenclature*. **2001**, 4
- [10] Westphal, E.; Mezger, T. *The Rheology Handbook. Vincentz Network*. **1996**, pg 97
- [11] Reologica Instruments. (2008) *Principles of Rheology*. Comprehensive Rheology Solutions: Retrieved February 26, 2008, from <http://www.reologcainstruments.com>
- [12] Ye, Z.; Zhu, S. *Macromolecules*, **2003**, 36, 2194
- [13] Widener University (2007). *NMR Experimental Techniques*. Retrieved April 4, 2008, from <http://science.widener.edu/svb/nmr/experiments.html>

[14] Salamone, J. *Polymeric Materials Encyclopedia*. CRC Press: **1996**

[15] Zhou, W.; Zhu, S. *Macromolecules* **1998**, 31, 4335

[16] Qu, B.; Qu, X; Xu, Y.; Jacobsson, U.; Ranby, B.; Russell, K.; Baker, W.  
*Macromolecules* **1997**, 30, 14

### **Chapter 3: Maleic Anhydride Grafting of Hyperbranched Polyethylene**

#### 3.1 Introduction

Grafting occurs when a pre-polymer (e.g. HBPE) with internal double bonds or abstractable protons is processed together with other saturated or unsaturated compounds (e.g. MAH). The compound grafted onto the polymer backbone is responsible for the property enhancement. Different methods have been proposed in the literature for MAH modification of polyolefins including: solution, melt, and solid-phase. Solution based reactions have the advantage of having the polymer and monomer usually soluble forming a homogeneous medium. On the contrary, grafting in melt is much faster, volume effective, and free of solvent recovery, which renders melt grafting more industrially appealing [1].

Success of grafting is commonly measured in terms of grafting density, and reaction efficiency. Grafting density is the fraction of the monomer that is grafted onto the polymer backbone as opposed to the fraction unused or lost to undesirable side reactions, and is typically quantified through titrations. Reaction efficiency, on the other hand, is the moles of monomer grafted with respect to the moles of initiator-generated radicals [2].

Grafting is typically the desired reaction from peroxide-initiated functionalization; however, other side reactions have been reported besides grafting. Such reactions include chain scission, crosslinking, and homopolymerization. For example, polyethylenes are

susceptible to branching or crosslinking caused by radical recombination, which results in the formation of gels or partially insoluble products. On the other hand, polypropylene is prone to degradation by  $\beta$ -scission of the formed radical [2]. Hyperbranched polyethylene has an extensive amount of branching, but has few linear chains, which makes it inclined to both side reactions.

While there are many papers published on the reaction of maleic anhydride with polyethylene, polypropylene, and ethylene-propylene copolymer, no known work has examined the peroxide-initiated MAH functionalization of HBPE. The target of this chapter is to functionalize HBPE with MAH and investigate the effect of temperature, initiator type, initiator concentration, and monomer concentration on the grafting density and reaction efficiency.

## 3.2 Experimental

### 3.2.1 Materials

Hyperbranched polyethylene (HBPE) with a molecular weight of 100,000 g/mol was kindly supplied by Dr. Zhibin Ye's Group – University of Laurentian, Ontario, Canada. It was synthesized using a Pd-diamine catalyst system at 35 °C, and ethylene pressure of 1 atm, according to the literature procedure [3]. Maleic anhydride (MAH) - 99% purity, dicumyl peroxide (DCP) - 98% purity, benzoyl peroxide (BPO) - 97% purity, potassium hydroxide, phenolphthalein indicator, and thymol blue indicator were

purchased from Aldrich. Xylene and hydrochloric acid (0.01 N) solution were supplied by Fisher Scientific.

### 3.2.2 HBPE-g-MAH Synthesis

Hyperbranched polyethylene (0.1 g) was dissolved in a 10 mL xylene solution in a round bottom flask at 130 °C for 20 minutes under a nitrogen blanket. MAH and DCP, in their solid form, were added to the solution after 20 minutes and the grafting reaction was allowed to proceed for 1 hour under a nitrogen blanket. Upon completion of the reaction, the hot solution was filtered using cheesecloth to remove the xylene-insoluble polymer. The filtrate was subsequently added to a 10-fold volume of acetone to precipitate the xylene-soluble polymer. As soon as the xylene-soluble polymer settled, the solvent was decanted, and the precipitated polymer was allowed to dry over night at room temperature. Subsequently, the polymer was dried in a vacuum oven at 110 °C for 12 hours to remove the residual solvent and any unreacted MAH.

### 3.2.3 Titration of Anhydride Content

The anhydride content was found by dissolving a fixed amount of HBPE-g-MAH in refluxing water saturated xylene for 1 hour. The hot solution was titrated immediately with a standard (~0.05 M ethanolic KOH using thymol blue (1 wt.%) in DMF as an indicator). The acid number and MAH content are calculated as follows [4]:

$$\text{acidnumber}(\text{mgKOH} / \text{g}) = \frac{m\text{LKOH} \times N\text{KOH} \times 56.1}{g\text{polymer}}$$

$$MAH(\%) = \frac{acidnumber \times 98}{2 \times 561}$$

Where  $mLKOH$  is the volume in mL of potassium hydroxide needed to reach the titration endpoint,  $NKOH$  is the molarity in mg/mL of potassium hydroxide solution used,  $g_{polymer}$  is the amount in g of HBPE-g-MAH dissolved in each aliquot of solution used in titration, and  $MAH(\%)$  is the percentage grafting density. Molecular weights of potassium hydroxide and maleic anhydride are 56.1 g/mol and 98 g/mol respectively. A blank experiment and three repeats were performed for every variation in concentration.

### 3.2.4 FTIR Characterization

FTIR spectra were recorded using Bio-Rad FTS-40 FTIR machine by applying a small amount of viscous HBPE-g-MAH onto a sodium chloride disk. Spectra are recorded in the range of 1700 to 1900  $cm^{-1}$  with a 4  $cm^{-1}$  resolution and 24 scans.

### 3.2.5 $^1H$ -NMR Characterization

Samples were prepared by dissolving HBPE-g-MAH (5 wt.%) in 1 mL of deuterated o-dichlorobenzene at 120 °C for 1 hr to homogenize. Spectra (2400 scans) were recorded on a Bruker AV 300 MHz spectrometer at a temperature of 120 °C.

### 3.2.6 Water Contact Angle Measurements

Polyester films were cleaned by sonication in acetone for 30 minutes. Homogenous polymer solutions of HBPE and HBPE-g-MAH in xylene (5 wt. %) were

prepared by dissolving the polymer in xylene for 30 minutes at 80 °C. The polymer was casted onto cleaned polyester films by pipetting a drop or two of the polymer solution onto the films and allowing the solvent to evaporate forming a thin film.

The wettability of the surface was measured at room temperature using a Ramé-Hart NRL goniometer (Mountain Lakes, NJ), where a droplet of pure water was applied to the surface and the contact angle was measured.

### 3.3 Results and Discussion

#### 3.3.1 FTIR Characterization of Grafted Polymer

Figure 3.1 shows the FTIR spectrum of HBPE-g-MAH, prepared using 2 wt.% DCP and 2 wt.% MAH at 130 °C for 1 hr under a nitrogen blanket.

Two absorption bands are observed at 1784-1792  $\text{cm}^{-1}$  and around 1850  $\text{cm}^{-1}$  that account for grafted maleic anhydride. A weak asymmetric stretching carbonyl absorption band and a stronger symmetric stretching carbonyl absorption band usually lay in the vicinities 1850  $\text{cm}^{-1}$  and 1780  $\text{cm}^{-1}$  respectively. De Roover et al. proposed that the two overlapping absorption bands at 1784  $\text{cm}^{-1}$  and 1792  $\text{cm}^{-1}$  are due to poly(maleic) anhydride and succinic anhydride end groups, respectively [5].

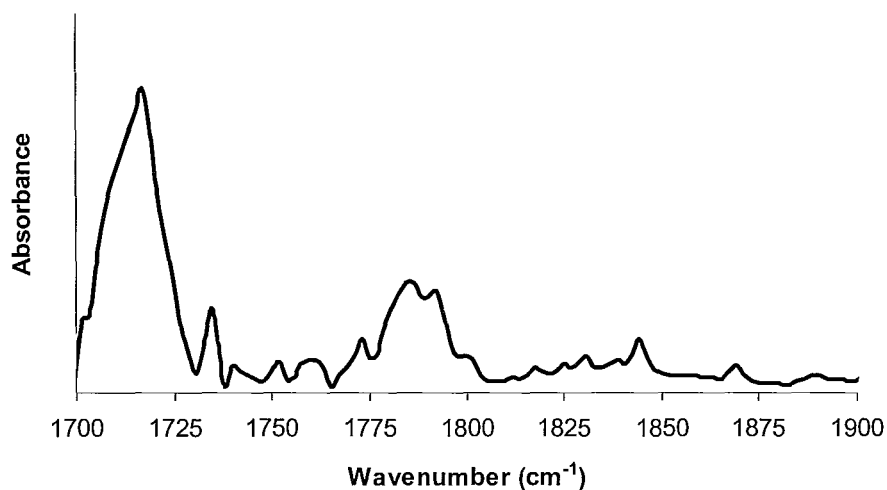


**Figure 3.1:** Infrared spectrum of HBPE-g-MAH in the range  $1700$  to  $1900\text{ cm}^{-1}$  prepared using 2 wt.% MAH, 2 wt.% DCP, and a reaction time of 1 hr at  $130\text{ }^{\circ}\text{C}$ . 24 scans were acquired with a resolution of  $4\text{ cm}^{-1}$ .

### 3.3.2 $^1\text{H}$ -NMR Characterization of Grafted Polymer

Figures 3.2 and 3.3 show the  $^1\text{H}$ -NMR spectra of peroxide initiated HBPE-g-MAH, prepared using 2 wt.% DCP and 2 wt.% MAH at  $130\text{ }^{\circ}\text{C}$  for 1 hr under a nitrogen blanket. Besides the expected  $\text{CH}_3$ ,  $\text{CH}_2$ , and  $\text{CH}$  peaks found at 0.89 ppm, 1.33 ppm, and 1.66 ppm respectively, other weak signals characteristic of the anhydride ring are apparent between 3 and 5 ppm.

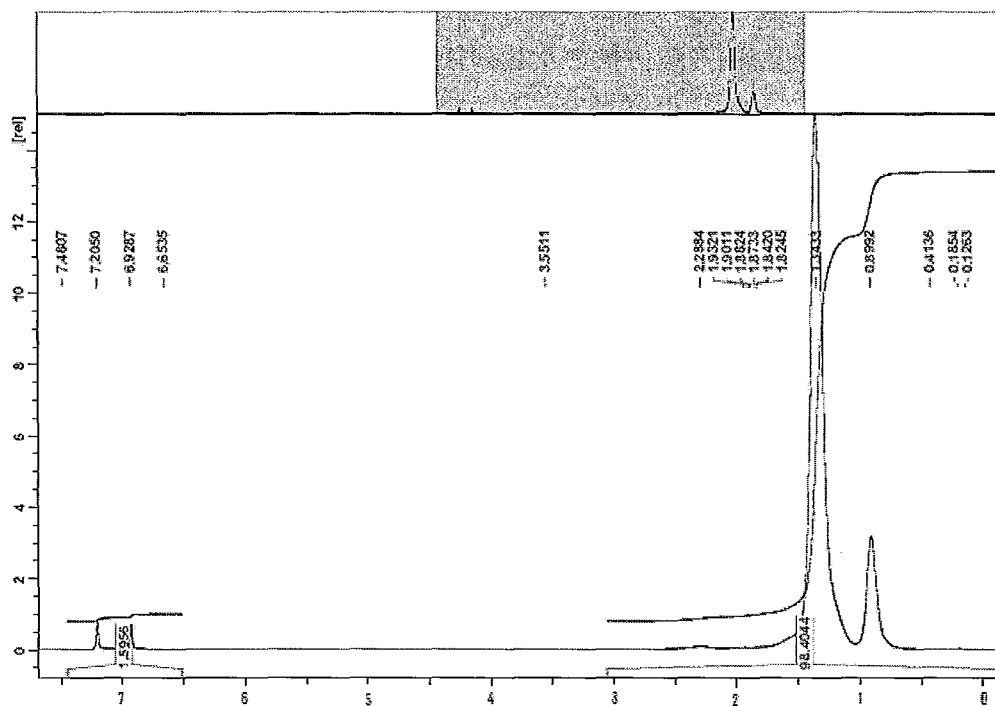


Figure 3.2:  $^1\text{H-NMR}$  of HBPE-g-MAH prepared using 2 wt.% DCP and 2 wt.% MAH at  $130\text{ }^\circ\text{C}$  for 1 hr.

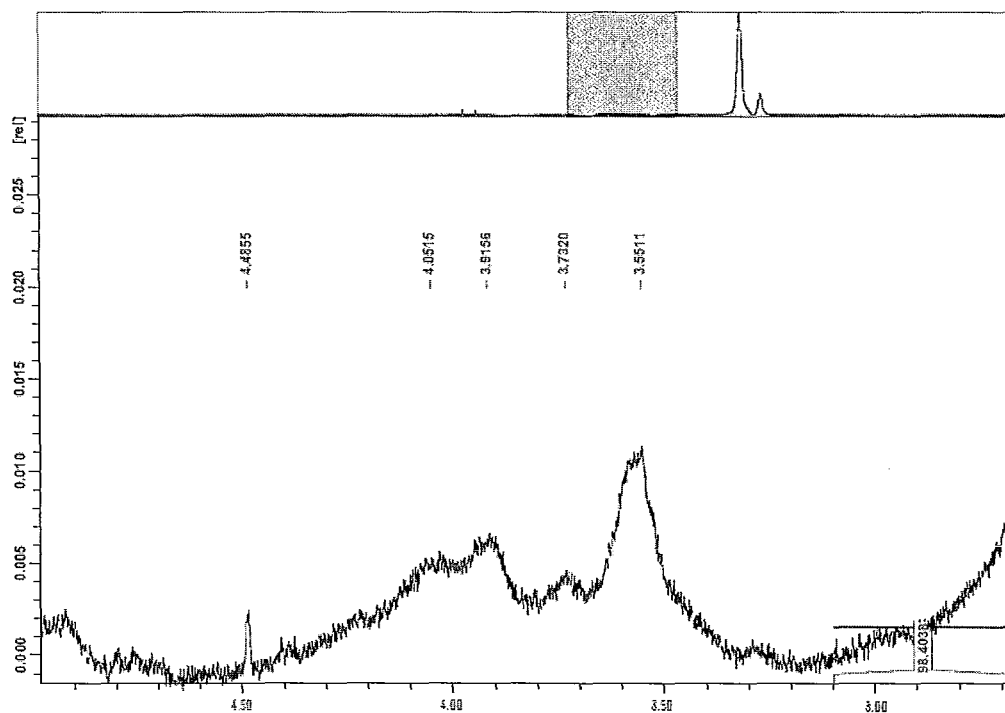
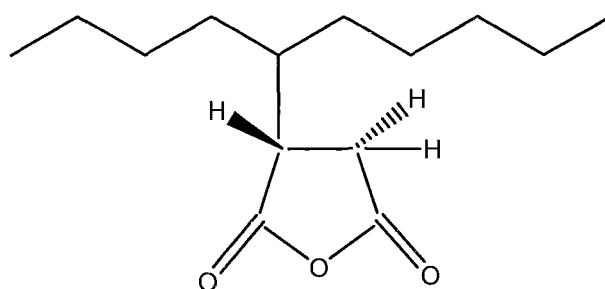
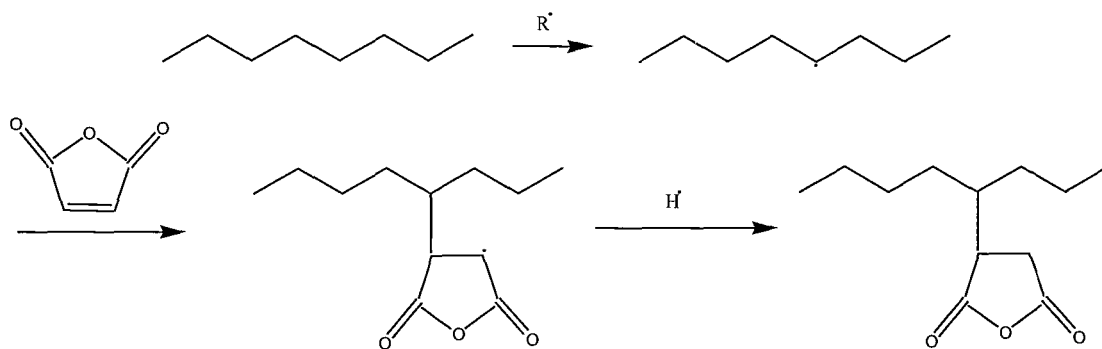


Figure 3.3:  $^1\text{H-NMR}$  of HBPE-g-MAH prepared using 2 wt.% DCP and 2 wt.% MAH at  $130\text{ }^\circ\text{C}$  for 1 hr.

The peaks at 3.73 ppm, 3.91 ppm, and 4.05 ppm could be assigned to the methyne proton and two methylene protons of the succinic anhydride ring grafted on the polymer side chain, as shown in Figure 3.4. The following graft structure is formed as a result of the reaction of the side chain radicals formed by peroxide initiation with maleic anhydride as shown in Figure 3.5.



**Figure 3.4:** Structure formula representing the methyne and two methylene protons of the succinic anhydride ring grafted on the polymer backbone [6].



**Figure 3.5:** Reaction route for the formation of the graft structure displayed in Figure 3.4 [7].

The small peaks at 3.25 ppm and 3.73 ppm could be assigned to the two methylene protons of the succinic anhydride ring grafted on the polymer side chain as

shown in Figure 3.6. This graft structure is formed as a result of the tertiary carbon radicals produced by peroxide initiation reacting with maleic anhydride forming the side chain grafted product (Figure 3.6), through  $\beta$ -scission [7]; reaction route is displayed in Figure 3.7.

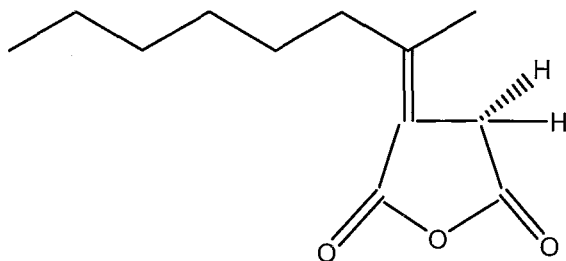


**Figure 3.6:** Structure formula representing the two methylene protons of the succinic anhydride ring grafted on the polymer backbone [6].

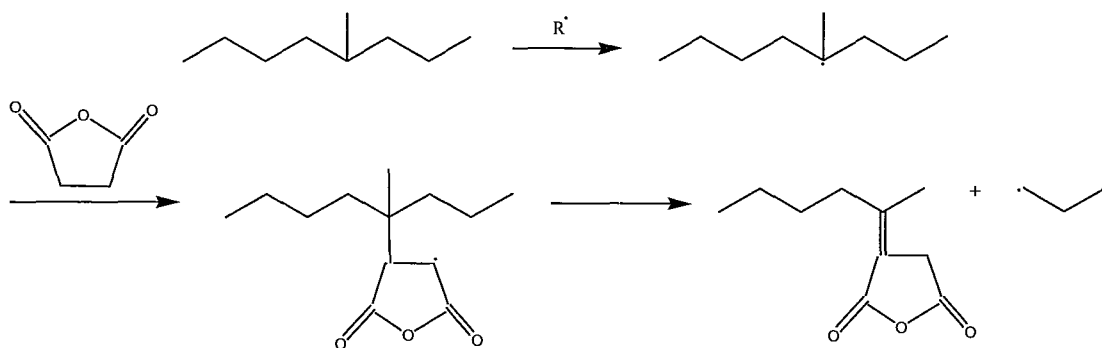


**Figure 3.7:** Reaction route for the formation of the graft structure displayed in Figure 3.6 [6].

The weaker peaks around 5.20 ppm correspond to the two hydrogens at the chain end of the succinyl terminated HBPE, which is shown in Figure 3.8.

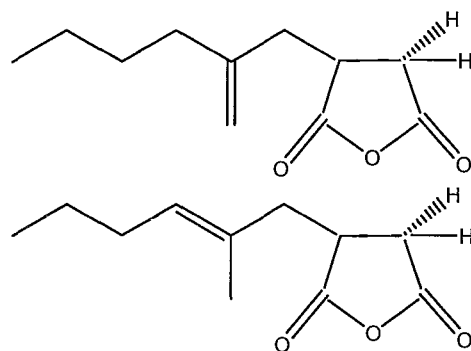


**Figure 3.8:** Structure formula showing the two hydrogens at the chains end of the succinyl terminated HBPE [7].

The sharp peak at 4.485 ppm could be assigned to the vinyl protons that originally existed in HBPE [6].

### 3.3.3 Effect of Initiator Type on Grafting Density

Dialkylidic peroxides are typically used for grafting reactions because of their stability and half-lives. If a radical has a short half-life, very high local concentration of radicals is produced in a short time, which increases the probability of secondary reactions. Moreover, incomplete decomposition may result from a long initiator half-life leading to a reduced grafting efficiency and residual peroxide remaining in the solution upon the completion of the reaction [8]. Nonetheless, different initiators tend to favor different side reactions, and this depends on the type of initiator and on the structure of the polymer. For instance, DCP tends to have a higher crosslinking efficiency compared to BPO; 50% and 27%, respectively [9].

In this section, the effect of the type of initiator on grafting density and reaction efficiency was investigated. Two different initiators were examined, namely, dicumyl

peroxide, and dibenzoyl peroxide. Initiator (2 wt.%) was added in both cases and the reaction was allowed to proceed for 1 hr under a nitrogen blanket. BPO has a much shorter half-life at 130 °C and therefore the amount of initiator used after 1 hr was accounted for when calculating the grafting density and reaction efficiency. Typical half-lives of DCP and BPO at 130 °C are 104 and 1.2 mins, respectively. Although complete consumption of BPO occurs in 1 hr, DCP still gave a two-fold increase in grafting density and significantly higher reaction efficiency. This occurred because the higher reactivity of BPO diminishes its capacity to be dispersed within the solution of available MAH molecules before being consumed, and therefore a lower grafting density. Results of the effect of type of initiator on grafting density and reaction efficiency are summarized in Table 3.1. The grafting density and reaction efficiency results are the averages of three different trials while their respective errors represent one standard deviation.

**Table 3.1:** Effect of type of initiator on grafting density and reaction efficiency. Dicumyl peroxide (DCP) and dibenzoyl peroxide (BPO) were used as initiators. Reaction conducted at 130 °C using 2 wt.% MAH, 2 wt.% initiator, xylene solvent, and allowed to proceed for 1 hr under a nitrogen blanket.

Initiator Type	wt.% initiator	wt.% MAH	Grafting Density (%)	Error – GD (%)	Reaction Efficiency	Error (RE)
DCP	2	2	1.66	± 0.09	4.12	± 0.22
BPO	2	2	0.76	± 0.16	0.47	± 0.10

### 3.3.4 Effect of Reaction Temperature on Grafting Density

Figure 3.9 shows the effect of varying solution temperature on the grafting density of MAH onto HBPE. The grafting density results are the averages of three different trials while the error bars represent a one standard deviation.

The boiling point of xylenes restricted the experiments to below 139 °C. Experiments were conducted at five different temperatures: 110, 115, 120, 125, and 130 °C, respectively. An increase in grafting density was observed at higher reaction temperatures. This effect is attributed to escalated initiator thermal decomposition rates at higher temperatures, which results in increased radical concentrations in solution. The formed radicals abstract hydrogen from the HBPE backbone, which increases the probability of MAH appendage and hence results in higher grafting densities.

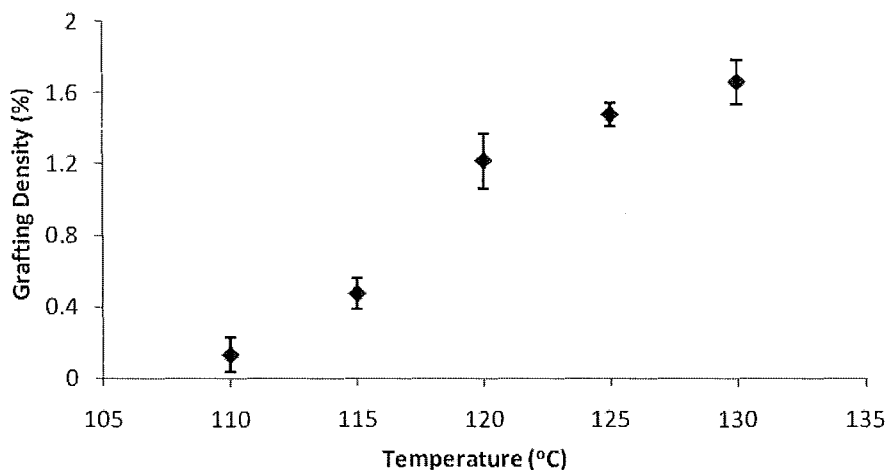


**Figure 3.9:** Effect of reaction temperature on grafting density. The reaction was conducted using 2 wt.% DCP, 2 wt.% MAH, and xylene solvent for 1 hr under a nitrogen blanket. Temperatures in the range 110 – 130 °C were examined.

### 3.3.5 Effect of Initiator Concentration on Grafting Density

Figure 3.10 shows the effect of varying initiator concentration on grafting density and reaction efficiency. The grafting density and reaction efficiency results are the averages of three different trials while their respective error bars represent a one standard

deviation. Dicumyl peroxide was used as an initiator since it gave improved grafting densities and reaction efficiencies compared to benzoyl peroxide. The highest grafting density (1.7 %) was observed at a loading of 2 wt.% DCP. At a concentration of 3 wt.% DCP, grafting density dropped to 0.8 %. The optimum grafting density observed between 2 wt.% and 3 wt.% DCP loading results from a balance between the grafting reaction and other side reactions. Increasing the concentration of initiator increases the radical concentration, which results in more active sites at the HBPE backbone, favoring MAH attachment. However, very high initiator concentrations will lead to excessive amounts of radical termination as opposed to MAH grafting. In summary, crosslinking and grafting are enhanced as the initiator concentration is increased up to the point where termination of primary radicals causes lower reaction efficiencies, which agrees with the literature [10].

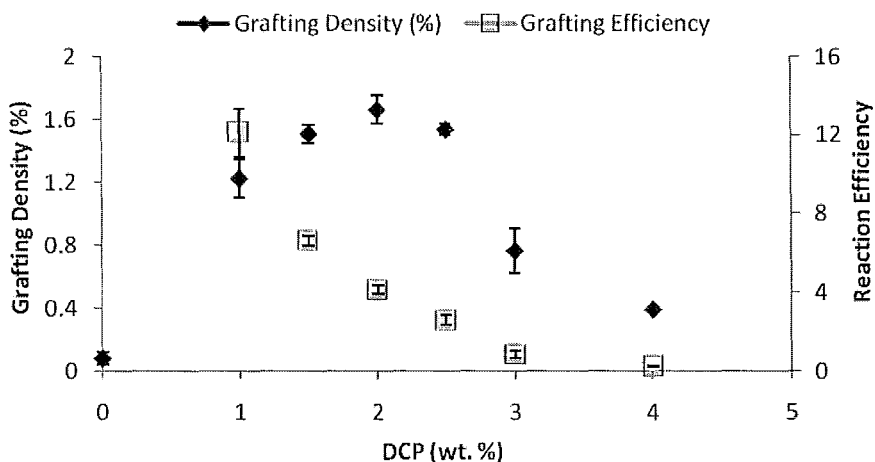


**Figure 3.10:** Effect of initiator concentration on grafting density and reaction efficiency. Reaction was conducted using dicumyl peroxide as an initiator, varying its concentration from 0 – 4 wt.%. Reaction was allowed to proceed for 1 hr, at 130 °C, under a nitrogen blanket using 2 wt.% MAH and xylene solvent.

### 3.3.6 Effect of Monomer Concentration on Grafting Density

Figure 3.11 shows the effect of varying monomer concentration on the grafting density, while maintaining a constant initiator concentration. The grafting density results are the averages of three different trials while the error bars represent a one standard deviation. As the amount of MAH added was increased, an increase in the grafting density was noticed, reaching a maximum at a monomer loading of 2 wt.%, followed by a plateau combined with a slight decrease in grafting density. The MAH in solution can either undergo homopolymerization, producing poly(maleic anhydride), or a thermal decomposition of the initiator molecules forming radicals that attack both the MAH monomer and HBPE. The macroradicals formed from initiator attacking HBPE backbone can undergo chain scission, or crosslinking leading to a decrease or increase in molecular weight [11].

The diffusion of the monomer molecules to the free radical sites controls the extent of grafting [12], therefore at low monomer concentrations, the amount of MAH in solution was insufficient to scavenge all radical sites produced on HBPE backbone. Moreover, the probability of homopolymerization is small. At higher MAH loading, increased appendage to HBPE backbone was expected, which is reflected by an increase in grafting density. At very high MAH concentrations, homopolymerization of MAH predominated over grafting; this leads to a decrease in the grafting density as seen in Figure 3.11.

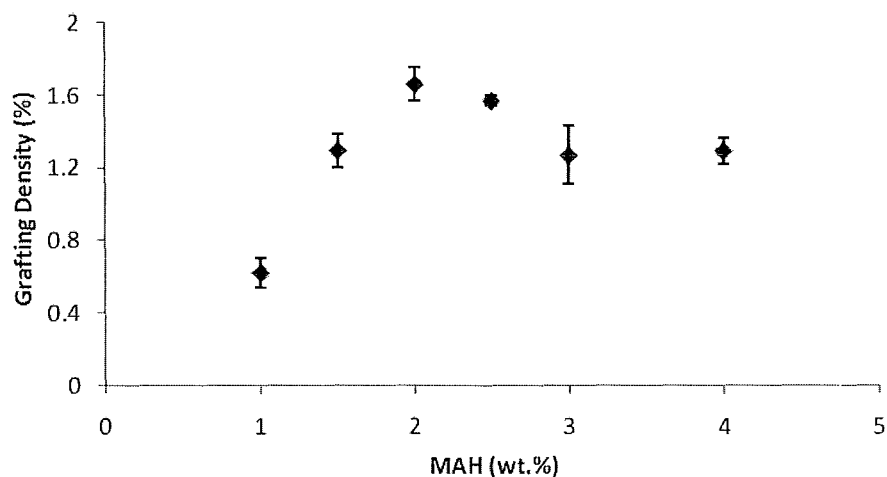


**Figure 3.11:** Effect of maleic anhydride concentration on grafting density. Maleic anhydride concentration was varied in the range 0 – 4 wt.%. Reaction was conducted at 130 °C for 1 hr under a nitrogen blanket, using 2 wt.% DCP, and xylene solvent.

### 3.3.7 Water Contact Angle Results

Table 3.2 shows that as HBPE is modified with MAH, the water contact angle decreases. Thin films of HBPE and HBPE-g-MAH were casted onto polyester films and the water contact angle was measured; the water contact angle results are the average of three different trials while the error associated represents a one standard deviation.

Unmodified HBPE exhibited a high water contact angle of 116° as expected for this hydrophobic material. A drop in water contact angle was noted for the grafted HBPE. The water contact angle for HBPE, synthesized using 2 wt.% DCP, and 3 wt.% MAH with a grafting density of 1.27 % was 91°, and the water contact angle for the one synthesized using 2 wt.% DCP, and 2 wt.% MAH, with a grafting density of 1.66 % was 87°.

A small amount of MAH grafting (1 %) onto HBPE backbone resulted in a significant drop in water contact angle. This was attributed to the polar character introduced to HBPE, through the appendage of MAH. Increase in grafting density resulted in further, but not as significant, decrease in water contact angle. Appendage of MAH onto HBPE backbone improved the compatibility of this polymer with polar substrates.

**Table 3.2:** Water contact angle results for HBPE, (2 wt.% DCP, 3 wt.% MAH) HBPE, and (2 wt.% DCP, 2 wt.% MAH) HBPE. Samples were prepared by casting a thin film onto a polyester film, applying a water droplet and measuring the water contact angle.

Grafting Density (%)	wt. % MAH	wt. % DCP	Water Contact Angle	Error in Water Contact Angle
0	0	0	116	± 3
1.27	3	2	91	± 2
1.66	2	2	87	± 2

### 3.4 Conclusion

Peroxide-initiated maleation of hyperbranched polyethylene elucidated that reaction temperature, initiator type, initiator concentration, and monomer concentrations have a great impact on grafting density and reaction efficiency.

Grafting of MAH on to HBPE backbone was successful as confirmed by FTIR and <sup>13</sup>C-NMR, and a maximal grafting density of 1.7 % was observed for HBPE-g-MAH prepared using 2 wt.% MAH and 2 wt.% DCP.

Comparing two different initiators, DCP and BPO respectively, DCP gave a significantly higher grafting density. Monomer concentration had a complex effect on grafting density, where the grafting density increased to a maximal value at 2 wt.% MAH concentration, after which it slightly decreased and leveled off. The observed effect is attributed to the competition between the grafting reaction, and other side reactions, where their dominancy changed depending on the concentration of MAH in the reaction medium. Grafting density increased with increased initiator concentration up to a critical concentration, followed by a noticeable drop due to radical-radical combination. Temperature increased the rate of initiator thermal decomposition, which subsequently resulted in higher grafting density.

Water contact angle measurements showed that functionalization of HBPE with MAH introduced a polar nature to the polymer, which was characterized by a significantly lower contact angle compared to unmodified HBPE. This makes HBPE-g-MAH compatible with polar substrates.

### 3.5 References

- [1] Machado, A.; Covas, J.; van Duin, M. *Polymer* **2001**, 42, 3649
- [2] Moad, G. *Prog. Polym. Sci.* **1999**, 24, 81
- [3] Ye, Z.; AlObaidi, F.; Zhu, S. *Macrom. Chem. Phys.* **2004**, 205, 897
- [4] Gaylord, N.; Mehta, R.; Kumar, V.; Tazi, M. *J. Appl. Polym. Sci.* **1989**, 38, 359

- [5] De Roover, B.; Scalvons, M.; Carlier, V.; Devaux, J.; Legras, E.; Momtaz, A. *J. Polym Sci: Polym Chem.* **1995**, 33, 829
- [6] Zhang, Y.; Chen, J.; Li, H. *Polymer* **2006**, 47, 4750
- [7] Shi, D.; Yang, J.; Yao, Z.; Wang, Y.; Huang, H.; Jing, W.; Yin, J.; Costa, G. *Polymer*, **2001**, 42, 5549
- [8] Krause-Sammartino, L.; Lucas, J.; Reboredo, M.; Aranguren, M. *Plastics, Rubber and Composites* **2006**, 35, 117
- [9] van Drumpt, J. *Rubber World*, **1988**, 33
- [10] Liu, N.; Baker, W., Russell, K. *J. Appl. Polym. Sci.* **1990**, 41, 2285
- [11] Guldogan, Y.; Egri, S.; Rzaev, Z.; Piskin, E. *J. Appl. Polym. Sci.* **2004**, 92, 3675
- [12] Wu, C.; Liao, H.; Lai, S. *Polym. Plast. Tech. Eng.* **2**

## **Chapter 4: Rheological Characterization of HBPE and HBPE-g-MAH**

### 4.1 Introduction

#### 4.1.1 Rheology

Rheology comes from the Greek work *rheos* meaning to *flow*, and it is the study of deformation and flow of matter subjected to a stress, which may be a shear stress or an extensional stress. The interest in rheology escalated with industrialization, as the flow, product quality, and production efficiency need to be controlled, which resulted in the wide use of rheological studies in various industries including food, paint, cosmetics, ceramic, pharmaceutical, and biotechnology. Materials rheological properties affect every phase of their production starting with process design, processing, quality control, and product development to product structure, and consumer acceptance (1). Additionally, rheology plays a vital role in the correlation string from the catalytic polymerization and chain structure to the processing behavior and end-use properties. Figure 4.1 shows the mutual effects of rheological parameters on molecular structure and processing behavior (2).

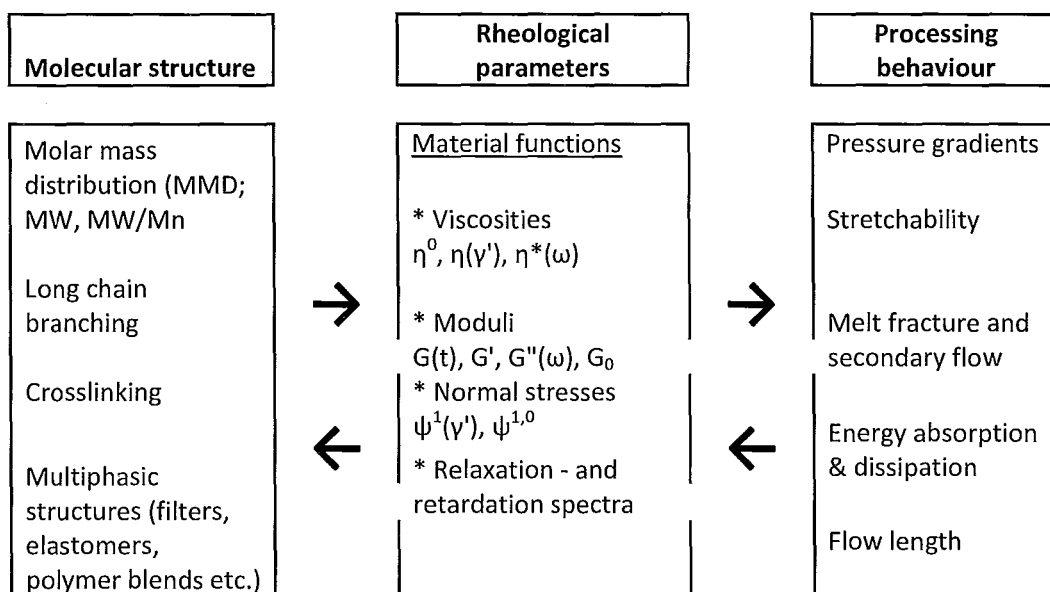


**Figure 4.1:** Schematic illustrating the link between rheological parameters and the molecular structure and processing behavior of a material (2).

#### 4.1.2 Theoretical Concepts in Rheology

Table 4.1 summarizes the terms, which are most frequently used when dealing with rheological properties and measurements:

**Table 4.1:** Definition of the most commonly used rheological terms.

Property	Definition	Symbol	Unit
<i>Stress</i>	Force per unit area	$\sigma$	Pa
<i>Shear</i>	Relative deformation	$\gamma$	Dimensionless
<i>Shear rate</i>	Change of shear strain per unit time	$\dot{\gamma}$	$s^{-1}$
<i>Viscosity</i>	Material resistance to flow	$\eta$	Pa.s

A material, depending on its flow behavior, generally belongs to one of the following categories: viscous, elastic, plastic, and viscoelastic. Viscosity is a measure of the resistance to flow, where a larger resistance corresponds to higher viscosity. A

viscous material flows when a force is applied, and this flow ceases once the force is removed, where a dashpot is typically used to represent a purely viscous response. Elastic materials, on the other hand, do not flow, but show solid-like properties. They are typically described as a spring, which follows Hooke's law of elasticity. According to Hooke's law, as a larger force is applied, a larger spring deformation results, and the spring restores its original shape once the applied force is removed. Plastic materials show flow properties in the same way as viscous samples, however flow occurs initially after a threshold shear stress is exceeded (i.e. yield stress), and the flow will cease as soon as the force applied is lower than the yield stress. Viscoelastic materials exhibit both elastic and viscous properties, and the response generally depends on the time scale of the experiment ( $t$ ), as opposed to the time scale of the sample, namely, the relaxation time ( $\tau$ ) (3).

The rheological behavior of a material is usually presented in two types of diagrams. One is the flow curve that shows the shear stress as a function of the shear rate, and the other is the viscosity curve, which shows the viscosity as a function of the shear rate (4).

#### 4.1.3 Characterization of Liquids

Liquids are generally categorized according to their shear rate dependency, which creates two categories of fluids, namely, Newtonian and Non-Newtonian (1).

### *Newtonian Liquids*

A material is Newtonian when the viscosity is constant and independent of shear rate, and the viscosity does not change with shearing time. This implies that as soon as the applied stress is zero, the shear rate is zero. The flow and viscosity curves for a Newtonian material are shown in Figure 4.2.

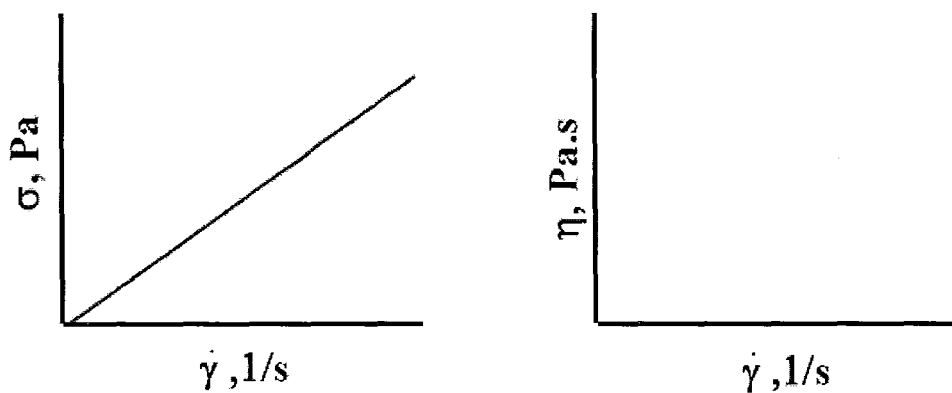


**Figure 4.2:** Typical flow and viscosity curves of a Newtonian material (4).

### *Non-Newtonian Liquids*

Non-Newtonian liquids are materials which exhibit a shear rate and/ or time dependency, and hence a non-constant viscosity. Therefore, these materials are generally divided into time-independent and time-dependent liquids. The materials which are used in this study are all time independent and therefore only time independent materials are discussed in this section.

Time Independent Materials:

a) Shear Thinning

This is a class of materials, which when subject to an increasing shear rate, the viscosity decreases, accompanied by a less than proportional increase in stress as shown in Figure 4.3.

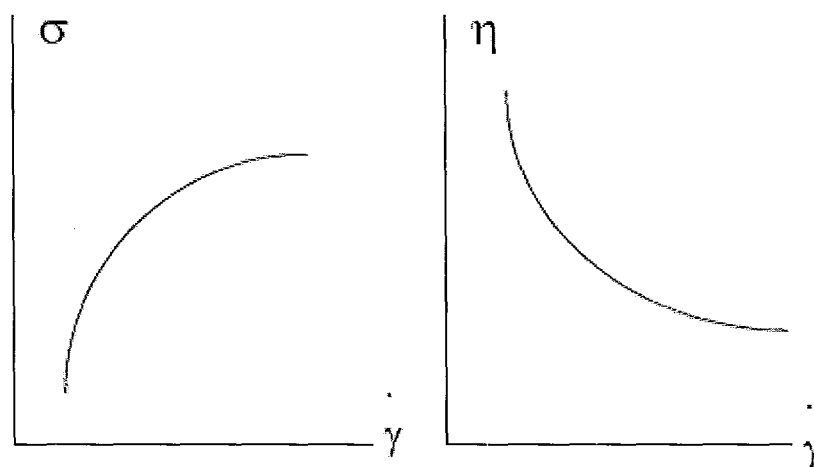


**Figure 4.3:** Typical viscosity and flow curves of a shear thinning material (3).

Shear thinning is mainly a characteristic of materials that contain some form of particles or chain coils, such as dispersions, emulsions, polymer melts and solutions. When shearing starts, the samples resistance to flow is reduced by the alignment of the asymmetric particles in the direction of the flow in the case of suspensions, or large molecules being disentangled and stretched, which is the case in polymer melts. Moreover, spherical molecules are deformed and aligned along the streamlines, which is the case for emulsions. Shearing also results in the physical separation of the particles,

and hence a reduction in the particle-particle interaction, or in the destruction of the sample microstructure. All the aforementioned factors result in a reduction in viscosity with shear rate, i.e. shear thinning (1).

b) Shear Thickening

Shear thickening liquids are those where the viscosity increases with shear rate, accompanied with a more than proportion increase in stress as shown in Figure 4.4.

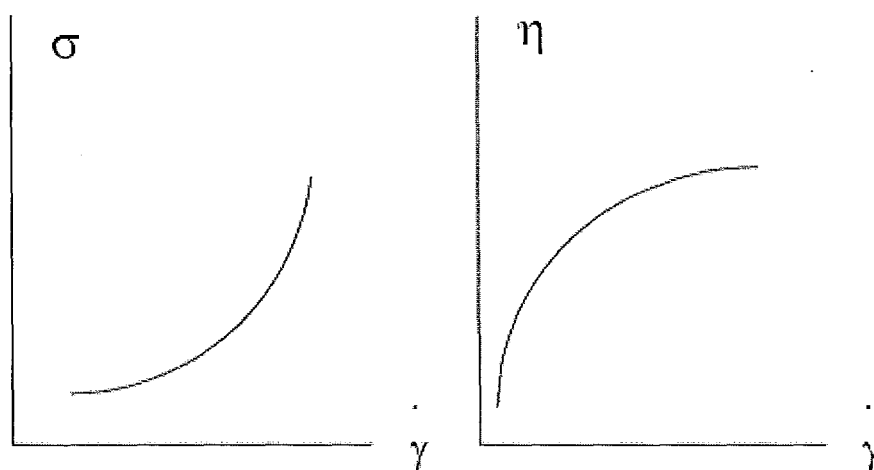


**Figure 4.4:** Typical viscosity and flow curves of a shear thickening material (3).

Highly concentrated suspensions are classified as shear thickening because at higher shear rates, the number of contact between particles increases, which increases the resistance to flow and hence the viscosity.

c) Yield Point

Those materials have to overcome a threshold stress known as the critical stress before they can exhibit any type of rheological behavior.

4.1.4 Rheological Behavior of HBPE

Hyperbranched polyethylene produced by a chain-walking mechanism at low ethylene pressure ( $< 1$  atm), relatively high temperature (25-35 °C), a Pd-diimine catalyst, was found to have many special features and properties, which have a great impact on its rheology. It was found that it exhibited dilute solution properties, a characteristic typical of dendrimers, and from neutron scattering (5) and AFM (5, 6, 7, 8, 9, 10) studies, it was also found to have a globular branched structure, similar to that of dendrimers but not as well defined and uniform, since it has a polydisperse molecular weight and branching-length distribution.

The aforementioned characteristics resulted in a viscous oil product, which exhibited a Newtonian behavior at various temperatures, and over a wide shear rate range. Ye et al. (11) reported this behavior for HBPE produced using a Pd-diimine catalyst at 35 °C, with an ethylene pressure of 0.2 and 1 atm, respectively (Figure 4.5).

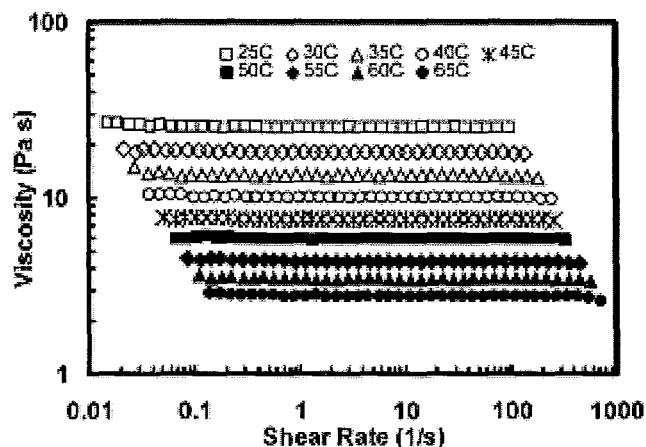


**Figure 4.5:** Steady shear viscosity as a function of shear rate for HBPE prepared at 35 °C, and 0.2 atm, using a Pd-diimine catalyst, measured at various temperatures (11).

#### 4.1.5 Scope and Objective

The scope of this chapter is to measure the rheological behavior of hyperbranched polyethylene grafted with maleic anhydride (HBPE-g-MAH), and that of its parent polymer (HBPE), using steady-shear, creep recovery, and dynamic oscillation tests.

The purpose of this study is to investigate whether the Newtonian behavior exhibited by pure HBPE and described in Section 4.1.6 is maintained upon grafting, or whether maleic anhydride grafting of the polymer would create a new set of rheological properties.

## 4.2 Experimental

### 4.2.1 Materials

HBPE with a molecular weight of 100,000 g/mol was kindly supplied by Dr. Zhibin Ye's Group – University of Laurentian, Ontario, Canada. It was synthesized using a Pd-diamine catalyst system at 35 °C, and ethylene pressure of 1 atm, according to the literature procedure (12). HBPE-g-MAH was prepared using 2 wt.% MAH and 2 wt.% DCP for 1 hr at 130 °C, under a nitrogen blanket (following the experimental procedure provided in Chapter 3).

### 4.2.2 Rheological Characterization

Rheological characterizations were conducted on a Stresstech HR rheometer in a 25 mm parallel plate mode with a gap of 1.0 mm. Experiments were performed at 10 °C intervals, in the range of 25 to 65 °C, while maintaining the temperature within  $\pm 0.2$  °C. Polymer samples were subject to steady shear, creep recovery, and small-amplitude dynamic oscillation in the controlled stress-mode, where three orders of magnitude of shear rates were covered. In the creep recovery experiments, samples were subject to a stress at time zero, and the compliance was monitored at constant stress for 100 s. The stress was subsequently removed, and the relaxation behavior was recorded. A frequency range of 0.001 – 90 Hz was covered in the small amplitude dynamic oscillation mode. Strain sweeps were performed before frequency sweeps to establish the linear viscoelastic region, and all three measurements were conducted on the same loaded sample.

Sources of error in rheological experiments could be present due to the lack of grip or gaps between the sample and the plate, temperature non-uniformities, and deformation of the sample during the course of the experiment.

### 4.3 Results and Discussion

#### 4.3.1 Flow Curves for HBPE and HBPE-g-MAH

In order to compare the rheological behavior exhibited by HBPE-g-MAH to its parent polymer (HBPE), the steady shear viscosity as a function of shear rate was measured and the results are presented in Figure 4.6. HBPE displayed a Newtonian flow behavior over three orders of magnitude of shear rates, typical of hyperbranched polymers, where the viscosity was independent of the shear rate at all tested temperatures. The same observation was reported by Ye et al. (11, 12).

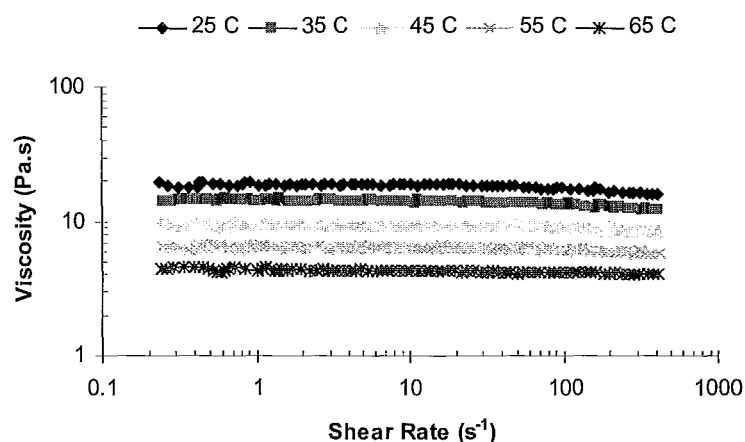


**Figure 4.6:** Steady shear viscosity as a function of shear rate for HBPE, measured at various temperatures in the range 25- 65 °C.

HBPE-g-MAH, exhibited the same behavior displayed earlier for HBPE, where the viscosity was independent of shear rate (Figure 4.7). However, data points obtained

below a shear rate of 10 Hz have been omitted due to the very low signal-to-noise ratio, as the material became more viscous upon grafting. Nevertheless, grafting with maleic anhydride resulted in an overall increase in viscosity at all tested temperatures, and also restricted the Newtonian flow behavior to a narrower window of shear rates, where it is apparent that some shear thinning occurs at high shear rates, for the lower measured temperatures; 25 °C to 45 °C, respectively. Although degradation by chain-scission is the dominant reaction for HBPE-g-MAH, and the material was found to be shear thinning, the overall viscosity of the grafted material increased instead of decreasing. However, this increase in viscosity is explainable in this case because the material has undergone solution fractionation during the grafting process, where the shorter chains were soluble in acetone, the solvent used in extraction, and therefore they left behind the longer chains, which in turn resulted in an overall increase in the viscosity of the grafted material.

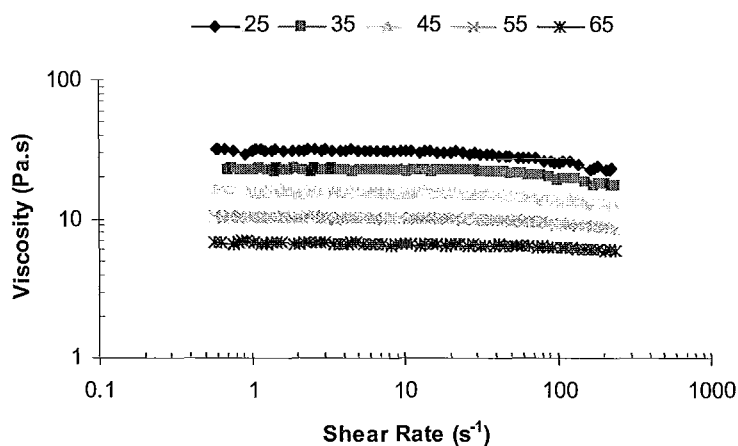


**Figure 4.7:** Steady shear viscosity as a function of shear rate for HBPE-g-MAH, measured at various temperatures in the range 25- 65 °C.

#### 4.3.2 Oscillation Measurement Results for HBPE and HBPE-g-MAH

The complex viscosity curves obtained from dynamic oscillation measurements conducted at various temperatures for HBPE and HBPE-g-MAH are shown in Figures 4.8 and 4.9, respectively.

Results obtained agree with findings from steady shear rate measurements for the same samples, and show a Newtonian flow behavior where complex viscosity is independent of frequency for HBPE, perhaps a small amount of shear thinning is observed for HBPE-g-MAH at the lower end of temperatures measured. Newtonian behavior observed in both steady shear and oscillatory measurements occurs due to the lack of chain entanglements between the polymer chains, where those chains can move past each other with ease and no restrictions. This is a result of dense packing of polymer molecules due to the hyperbranched chain topology and surface congestion, which prevented any chain entanglements (13). The shear thinning observed for HBPE-g-MAH at low temperature suggests that the extent of chain entanglements increases upon modification with maleic anhydride.

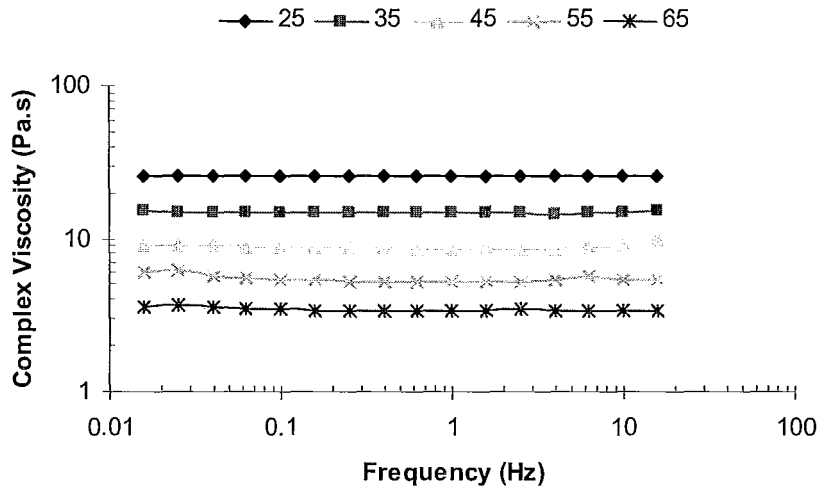


**Figure 4.8:** Complex viscosity as a function of frequency for HBPE, measured at various temperatures in the range 25- 65 °C.

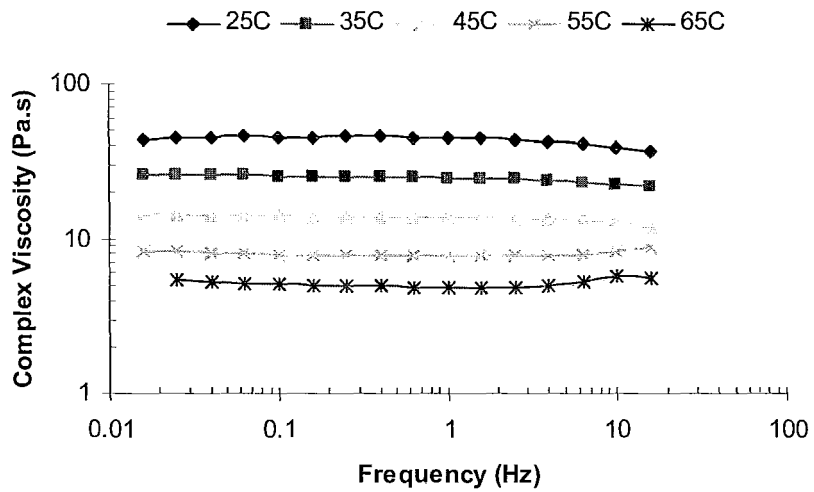


**Figure 4.9:** Complex viscosity as a function of frequency for HBPE-g-MAH, measured at various temperatures in the range 25- 65 °C.

### 4.3.3 Creep-recovery Results for HBPE and HBPE-g-MAH

Creep recovery measurements were used to investigate whether HBPE and HBPE-g-MAH behave as viscoelastic materials or show a pure viscous response, and whether modification by grafting has an effect on the compliance. The creep recovery curves are presented in Figures 4.10 and 4.11 for HBPE and HBPE-g-MAH, respectively.

All creep recovery curves display a behavior characteristic of viscous materials, where the strain increased constantly while the stress is applied, and remained constant once the stress was ceased, which illustrates an irreversible deformation. No elastic recovery has been observed for any of the curves tested at various temperatures, which elucidates that both HBPE and HBPE-g-MAH are purely viscous in nature, and modification by peroxide initiated grafting did not have any effect on the molecular structure of the material.

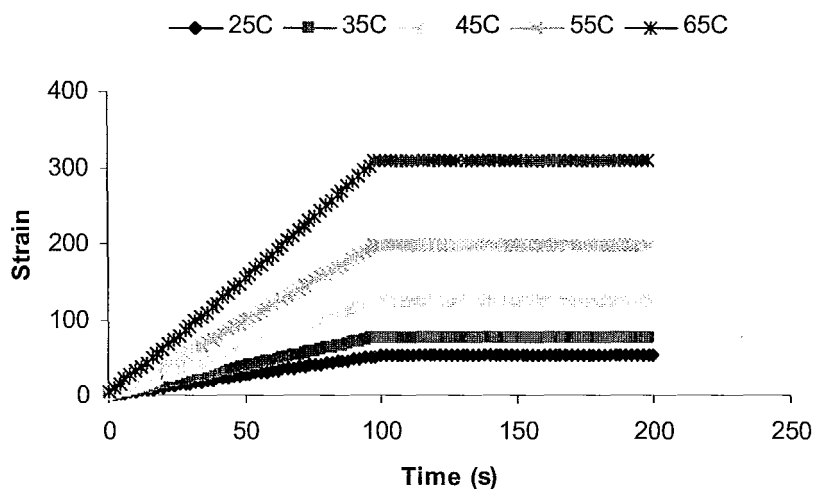


**Figure 4.10:** Compliance curve for HBPE obtained from creep-recovery experiment, measured at various temperatures in the range 25- 65 °C.

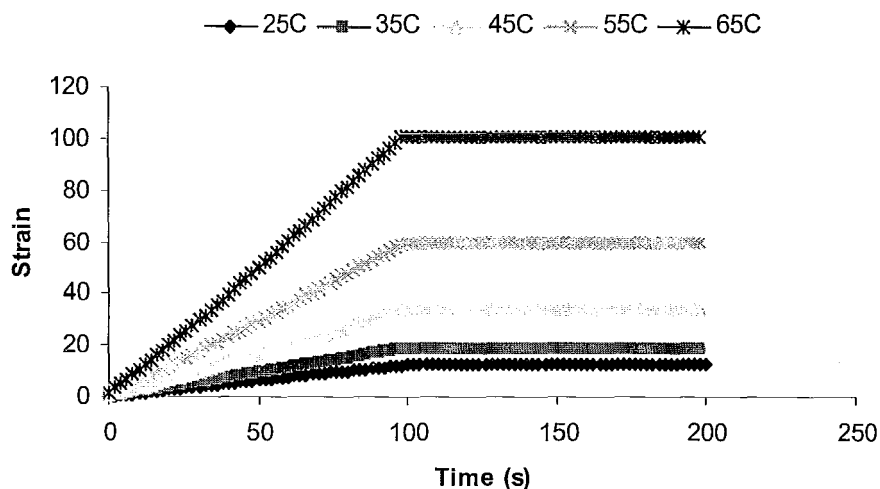


**Figure 4.11:** Compliance curve for HBPE-g-MAH obtained from creep-recovery experiment, measured at various temperatures in the range 25- 65 °C.

#### 4.4 Conclusion

This work identified the rheological attributes, which are characteristic of HBPE and HBPE-g-MAH. It was found that peroxide initiated modification of HBPE with maleic anhydride had a minute effect on the rheological properties of the parent polymer. HBPE-g-MAH maintained the same Newtonian behavior as HBPE upon grafting, which is typical of hyperbranched polymers, however, an increase in viscosity was noticed upon modification and slight shear thinning behavior was experienced at high shear rates for samples tested at low temperatures (25 – 45 °C).

This concludes that maleic anhydride grafting of HBPE, has no effect on the microstructure of the polymer, where the entanglements free environment due to the

globular and compact structure of the polymer was maintained, and resulted in a purely viscous material with Newtonian flow properties.

#### 4.5 References

- (1) REOLOGICA Instruments. *Reologica Rheometer Manual*, AB: **2000**, pg 91
- (2) Gahleitner, M. *Prog. Polym. Sci.* **2001**, 26, 895
- (3) Akzo Nobel. (**2002**) *Basic Rheology*. Retrieved January 7, 2008, from <http://www.cs.akzonobel.com/MarketSegments/Paint/Rheology.htm>
- (4) Reologica Instruments. (**2008**) *Principles of Rheology - Comprehensive Rheology Solutions*. Retrieved April 17, 2008, from <http://www.reologcainstruments.com>
- (5) Guan, Z.; Cotts, P. *Polym. Mat. Sci. Eng.* **2001**, 84, 382
- (6) Guan, Z. *Chem. Eur. J.* **2002**, 8, 3087
- (7) Guan, Z. *J. Am. Chem. Soc.* **2002**, 124, 5617
- (8) Guan, Z. *J. Polym. Sci.: Part A: Polym. Chem.* **2003**, 42, 213
- (9) Cotts, P.; Guan, Z.; McCord, E.; McClain, S. *Macromolecules* **33**, 6945
- (10) Guan, Z.; Cotts, P.; McCord, E.; McClain, S. *Science* **1999**, 283, 2059
- (11) Ye, Z.; Zhu, S. *Macromolecules* **2003**, 36, 2194
- (12) Ye, Z.; AlObaidi, F.; Zhu, S. *Macrom. Chem. Phys.* **2004**, 205, 897
- (13) Hawker, C.; Farrington, P.; Mackay, M.; Wooley, K.; Frechet, J. *J. Am. Chem. Soc.* **1995**, 117, 4409

## **Chapter 5: Crosslinking of HBPE-g-MAH**

### 5.1 Introduction

#### 5.1.1 Polymer Crosslinking

Crosslinking is the process of joining two or more chains by a direct link with covalent bond. The result of crosslinking is to restrict the movement of the polymer chains relative to each other, so that when heat and other forms of energy are applied, the network structure of the material prevents it from deforming, and material characteristics exhibited at room temperature are maintained at higher temperatures (1). Crosslinking can also be used to modify or enhance the polymer properties, to make it suitable for specific applications.

Polymer crosslinking can be achieved through multiple routes, including radiation treatment, such as ionization energy, electron beam processing, x-ray processing, and gamma processing, in which the radiation interacts with the polymer chain forming active sites necessary for the crosslinks to form. Another route is through chemical crosslinking, where chemicals such as peroxides are added to the polymer, or the chemical chain is chemically modified using, for example, silanes or maleic anhydride. After the desired product has been formed, an additional processing step, initiates a chemical reaction forming the active sites, and subsequently, the crosslinks; the most common processing step is exposure to heat (2).

Chemical crosslinking is used in this chapter to crosslink hyperbranched polyethylene pre-grafted with maleic anhydride, to investigate whether the crosslinked material would be suitable for reaction injection molding (RIM) applications.

### 5.1.2 RIM History

Reaction injection molding (RIM) technology for polyurethanes was developed by Bayer AG in the late 1960's. This technology, on the other hand, has been significantly improved since it was first developed to fit a wider range of end-use products and applications.

RIM is a plastics-forming process, which is not constrained to a resin with narrowly defined properties. Polyurethane RIM technology uses polyurethane to manufacture molded parts with different properties and applications. It can produce molds ranging from being very flexible to extremely rigid.

Most monomers forming other thermoplastics come in a pellet form, however polyurethane is composed of two different liquid monomer precursors: an isocyanate and a polyol. The properties of the final mold are dependent on how the isocyanate and polyol systems are formulated (3).

### 5.1.3 RIM Operation

Reaction injection molding is a chemical reaction by which two liquids are reacted together upon mixing to form a solid product. The two liquid components (polyol and isocyanate) are kept in two separate, agitator-equipped, and temperature-controlled vessels. Both components are fed in a precise manner, and at high pressure, through supply lines to a mixhead device.

Liquid reactants enter the mixhead at pressures ranging from 1500 to 3000 psi, where they are mixed intensively by high-velocity impingement. Mixed reactants flow from the mixhead to the mold at approximately atmospheric pressure, where they undergo an exothermic chemical reaction resulting in the polyurethane polymer. For an elastomeric part of an average mold size, the mold can be filled in less than a second, and it is ready for demolding in 30 to 60 seconds; however, the cycle and shot times are dependent on the size of the mold and the formulation of the reactants (3). A schematic representation for a polyurethane RIM system is shown in Figure 5.1.

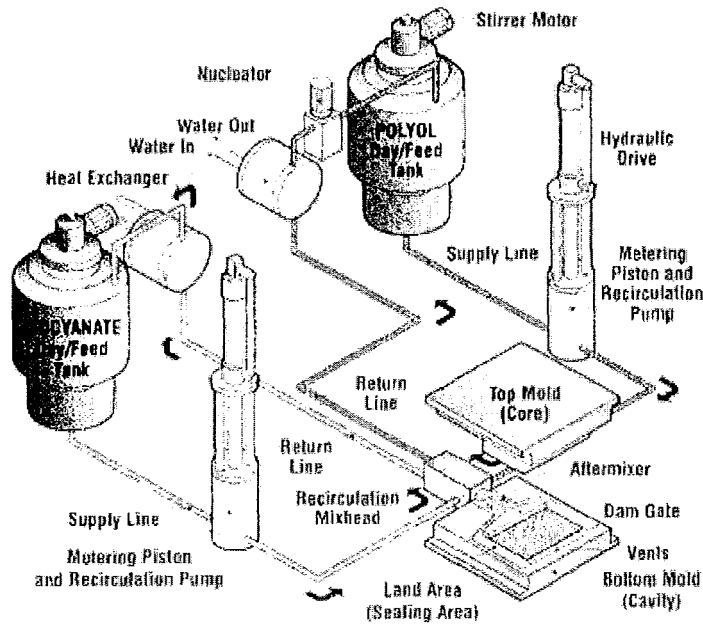


Figure 5.1: Reaction injection molding process schematic (4).

#### 5.1.4 Advantages of RIM

The unique advantages of RIM technology include:

1. Utilizing very low viscosity liquids ranging from 500 to 1500 centipoise,
2. Handling low processing temperature,
3. Handling low mold temperatures, and
4. Handling low internal mold pressures.

The low viscosity, low temperature, and low pressure provide some very distinct benefits for the RIM process compared to other plastic processing technologies (5).

### 5.1.5 Work Objective

The objective of this work is to examine whether HBPE-g-MAH could be used as a potential material for RIM applications. Solution amination is conducted to investigate the effect of temperature, reaction time, and diamine concentration on the degree of crosslinking of the resultant product. Melt amination is conducted to imitate industrial reaction injection molding conditions.

## 5.2 Experimental

### 5.2.1 Materials

HBPE-g-MAH was prepared using 2 wt.% MAH and 2 wt.% DCP for 1 hr at 130 °C under a nitrogen blanket (following the experimental procedure provided in Chapter 3). 1,8-Diaminooctane was purchased from Aldrich, while xylene solution was supplied by Fisher Scientific.

### 5.2.2 Solution Amination of HBPE-g-MAH

HBPE-g-MAH (0.1 g) was dissolved in a 10 mL xylene solution at 130 °C for 15 mins, under a nitrogen blanket, to achieve homogenization. Required amount of 1,8-diaminooctane was subsequently added to the mixture and amination reaction was allowed to proceed for 1 hr. Upon completion of the reaction, polymer was precipitated using 5-fold volume of acetone, which was further decanted as soon as the polymer settles. Finally, aminated HBPE-g-MAH was dried in a vacuum oven at 115 °C over night before measuring its gel content.

### 5.2.3 Melt Amination of HBPE-g-MAH

HBPE-g-MAH (0.5 g) and finely grinded 1,8-diaminooctane (4 mol 1,8-diaminooctane/ mol HBPE-g-MAH) were added in a layer form to a Petri-dish. The mixture was sonicated in a water-bath at room temperature for 1 hr to achieve intimate mixing. The Petri-dish was subsequently placed in a beaker, which in turn is submerged in an oil bath at 180 °C. The melt amination of HBPE-g-MAH was then allowed to proceed for 1 hr.

### 5.2.4 Gel Content Measurement

A weighed amount of aminated HBPE-g-MAH is added to a pre-weighed thimble, which is then inserted to a Soxhlet apparatus running under reflux for 24 hrs, where xylene is used as a solvent. After 24 hours, the thimble containing the gelled polymer is dried under vacuum at 60 °C for 12 hrs. Subsequently, the dried thimble is weighed and the gel content is calculated based on the amount of gelled polymer in the thimble with respect to the initial amount of polymer added to the thimble (6).

### 5.2.5 FTIR Characterization

FTIR spectra were recorded using Bio-Rad FTS-40 FTIR machine by applying a small amount of aminated HBPE-g-MAH onto a sodium chloride disk. Spectra were recorded in the range of 1650 to 1850  $\text{cm}^{-1}$  with a 4  $\text{cm}^{-1}$  resolution and 64 scans.

### 5.3 Results and Discussion

#### 5.3.1 FTIR Characterization of Crosslinked Polymer

The FTIR spectrum of aminated HBPE-g-MAH prepared using 4 mol 1,8-diaminooctane/ mol HBPE-g-MAH at 130 °C for 1 hr is shown in Figure 5.2. The absorption band around 1780  $\text{cm}^{-1}$  is characteristic of grafted maleic anhydride onto HBPE backbone (7). The new sharp peak introduced at 1700  $\text{cm}^{-1}$  was due to the formation of the imide group upon conducting the amination reaction (8).

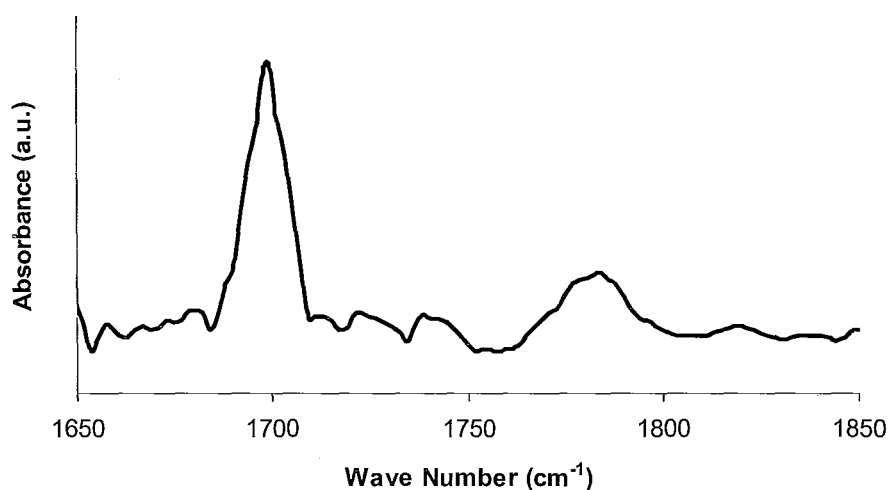


**Figure 5.2:** Infrared spectrum of diamine crosslinked HBPE-g-MAH between 1650 and 1850  $\text{cm}^{-1}$  crosslinked using 4 mol diamine/ mol HBPE-g-MAH, reaction time of 1 hr at 130 °C. 64 scans were acquired with a resolution of 4  $\text{cm}^{-1}$ .

#### 5.3.2 Effect of Reaction Temperature on Degree of Crosslinking

Figure 5.3 displays the effect of reaction temperature on the amination reaction of HBPE-g-MAH. Five different temperatures were investigated: 110, 115, 120, 125, and 130 °C, respectively. Reaction was allowed to proceed for 1 hr using 4 mol 1,8-

diaminooctane/ mol HBPE-g-MAH. It is noticeable that increasing the reaction temperature from 110 °C to 120 °C resulted in increasing the gel content of the crosslinked product from 52 % to 62 %. However, further increase in reaction temperature to 130 °C gave a gel content of 63%, which was consistent with that obtained at 120 °C. This shows that the degree of crosslinking was independent of reaction temperature beyond 120 °C.

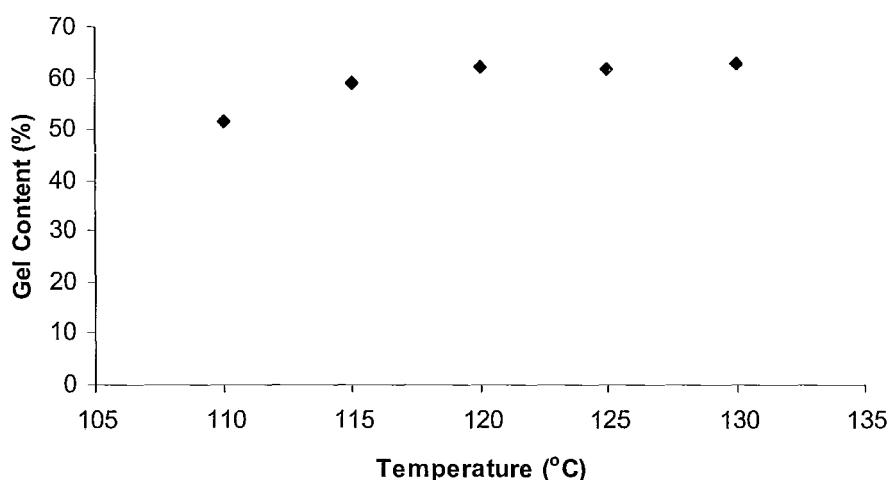


**Figure 5.3:** Effect of reaction temperature on the degree of crosslinking of HBPE-g-MAH. The reaction was conducted by adding 4 mol diamine/ mol HBPE-g-MAH, using xylene as a solvent under a nitrogen blanket. Reaction time was 1 hr and temperature was varied in the range 110 – 130 °C.

### 5.3.3 Effect of Reaction Time on Degree of Crosslinking

The effect of reaction time on the degree of crosslinking has been investigated, and the results are presented in Figure 5.4. Reaction time was varied from 1 to 4 hrs at 130 °C, using 4 mol 1,8-diaminooctane/ mol HBPE-g-MAH. Increasing reaction time from 1 to 4 hrs did not have a significant effect on the degree of crosslinking of aminated

HBPE-g-MAH. Running the reaction for 4 hrs resulted in a 67.1 % gelled polymer as opposed to 62.7 % achieved upon running the reaction for 1 hr. This proves that the effect of reaction time on solution amination of HBPE-g-MAH is minute beyond 1 hr, and therefore running the reaction for 1 hr is sufficient to achieve approximately the same level of crosslinking as running it for 4 hrs. This agrees with the findings of Lu et al. that the reaction of an aliphatic primary amine and a cyclic anhydride is very fast (8). From an industrial standpoint, although 4 hrs of reaction time gives a slightly higher degree of crosslinking, however the costs associated with conducting the reaction for 4 hrs as opposed to 1 hr, outweigh the advantage acquired from a slight increase in gel content.

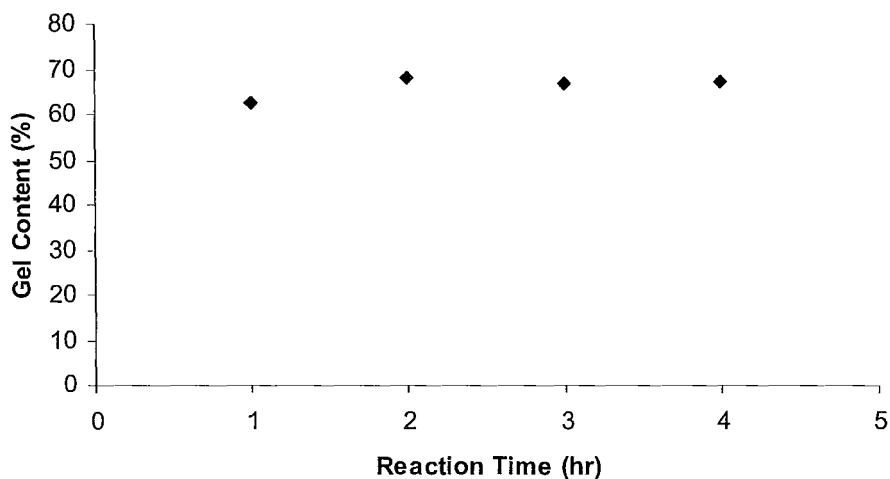


**Figure 5.4:** Effect of reaction time on the degree of crosslinking for HBPE-g-MAH. Reaction was conducted by adding 4 mol diamine/ mol HBPE-g-MAH, using xylene as a solvent under a nitrogen blanket. Reaction temperature was 130 °C and reaction time was varied from 1 – 4 hrs.

### 5.3.4 Effect of Diamine Content on Degree of Crosslinking

The amount of 1,8-diaminooctane was varied to examine its effect on the degree of crosslinking. Experiments were conducted at 130 °C for 1 hr under a nitrogen blanket, using 0 to 8 mol 1,8-diaminooctane/ mol HBPE-g-MAH. Gel content increased as the concentration of 1,8-diaminooctane was increased until it reached a maximal of 62.7 % at 4 mol 1.8-diaminooctane/ mol HBPE-g-MAH, where after this peak it started to decrease. In amination, there is a competition between two reactions depending on the concentration of diamine added; as can be shown in a structural schematic for the reaction (Figure 5.5). Initially, when the concentration of diamine is less than or equal to 4 mol 1.8-diaminooctane/ mol HBPE-g-MAH, HBPE-g-MAH chains will get linked to both converted functional groups of the diamine – reaction (b), as opposed to having free amine functionality attached to each HBPE-g-MAH molecule – reaction (a). Crosslinking results from the coupling of both diamine functional groups to two MAH groups on different HBPE chains, which leads to an increase in viscosity. Beyond 4 mol 1.8-diaminooctane/ mol HBPE-g-MAH, reaction (a) is dominant, where at least one free amine group is attached to each HBPE-g-MAH molecule, resulting in a decrease in the gel content.

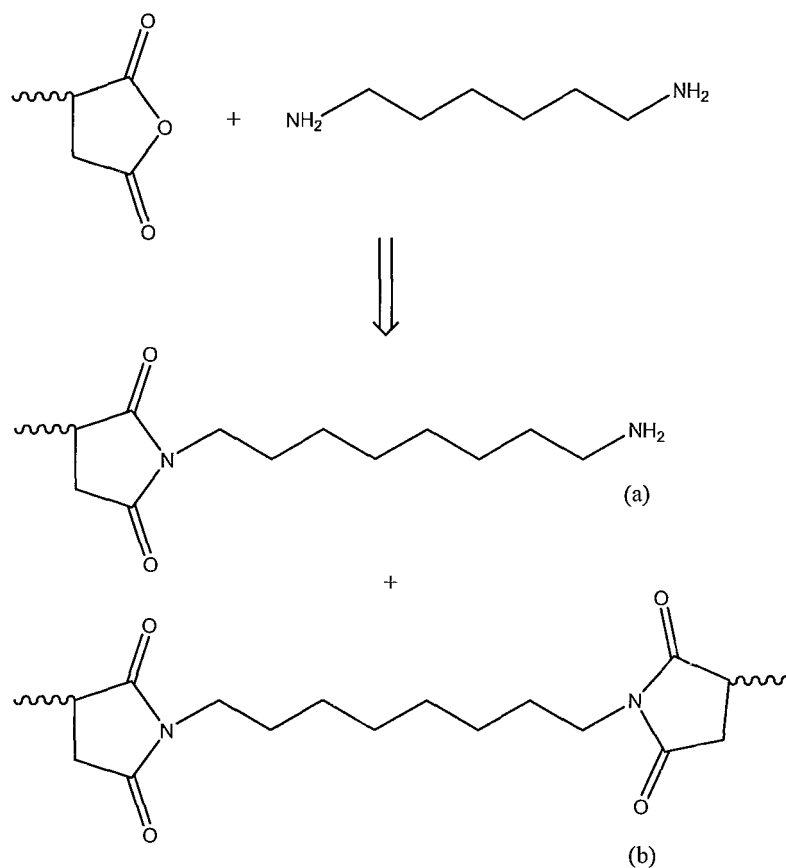


**Figure 5.5:** Reaction of diamine with hyperbranched polyethylene.

Lu et al. (8) reported the amination results for PP-g-MAH using hexamethylenediamine, which is a slightly shorter diamine than the one used in this study. They found that 0.5 mol hexamethyldiamine/ mol PP-g-MAH is the critical diamine concentration, where coupling of both functional groups occurs below this concentration – reaction (b), and attachment of free amines occurs above this concentration – reaction (a) (8). Comparing these results to those reported for HBPE-g-MAH (Figure 5.6) reveals a very important feature retaining to the effect of the structural

properties of these polymers on the critical concentration of diamine, and the point at which reactions (a) and (b) switch dominance.

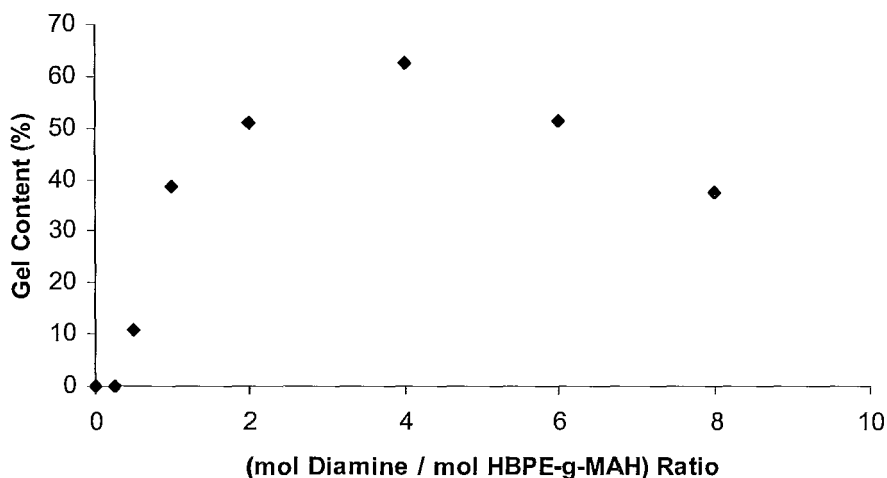


**Figure 5.6:** Effect of diamine concentration on the degree of crosslinking of HBPE-g-MAH. Reaction was conducted at 130 °C for 1 hr using xylene as a solvent under a nitrogen blanket. Diamine concentration was varied in the range 0 – 8 mol diamine/ mol HBPE-g-MAH.

The degree of branching of polymers controls the feasibility and extent of crosslinking. Statistically speaking, one diamine molecule should be sufficient to crosslink two polymer chains, however the structure of the polymer can render achieving this statistical ratio infeasible. Hyperbranched polyethylene is extremely branched, and globular in nature, which hinders the diffusion of diamine molecules, and makes it tougher to couple two different chains, due to limited accessibility of maleic anhydride moieties residing inside globular structure. Therefore, a high concentration of diamine is necessary to gel the polymer as can be seen in Figure 5.7 (a). Polypropylene, on the other hand, although branched (with CH<sub>3</sub> groups), still exhibits a linear structure, which makes

the diffusion of diamine molecules between the chains more facile and hence it is much easier to couple two different chains. Hence, a much lower concentration of diamine in solution is sufficient to cause crosslinking, and the statistical ratio mentioned earlier can be achieved as shown in Figure 5.7 (b).

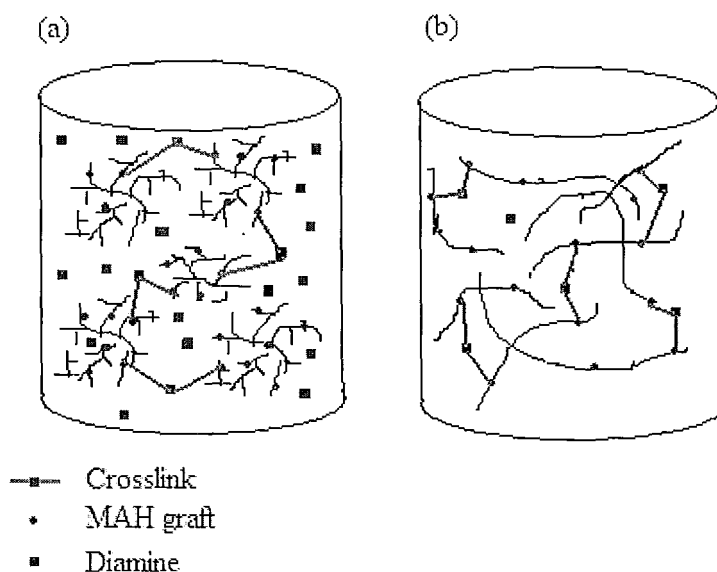


**Figure 5.7:** Illustration for the amination reaction of (a) HBPE and (b) PP.

### 5.3.5 Application to Reaction Injection Molding

Melt amination of HBPE-g-MAH was conducted to examine the feasibility of using this type of material in reaction injection molding applications. Figure 5.8 is a schematic of the process, where both HBPE-g-MAH (A) and 1,8-diaminoocatine (B) are mixed by sonication, and then heated to form a mold.

The amination reaction was conducted in melt at 180 °C for 1 hr to imitate reaction injection molding conditions. The resultant crosslinked polymer is shown in Figures 5.8 and 5.10, where snapshots were taken upon the completion of the reaction. Hyperbranched polyethylene is a viscous oil, and 1,8-diaminooctane has a melting point of 50–52 °C; both materials are in liquid form at the temperature at which the reaction is conducted. Melt amination was successful as both materials formed a soft solid material of aminated HBPE-g-MAH, with a degree of crosslinking of 70 %, which renders HBPE-g-MAH suitable for reaction injection molding applications upon crosslinking with an amine. The only drawback is the change in color accompanied by amination, where the polymer changes from colorless to a deep yellow color. This problem can be overcome by adding coloring reagents depending on the final use or application.

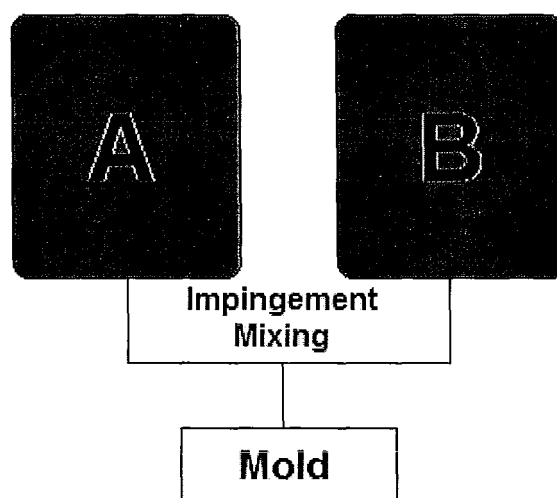


**Figure 5.8:** Process schematic for reaction injection molding (9).



**Figure 5.9:** Diamine crosslinked HBPE-g-MAH, prepared by using 4 mol diamine/ mol HBPE-g-MAH. Mixture was sonicated to achieve good mixing before conducting melt reaction at 180 °C for 1 hr.

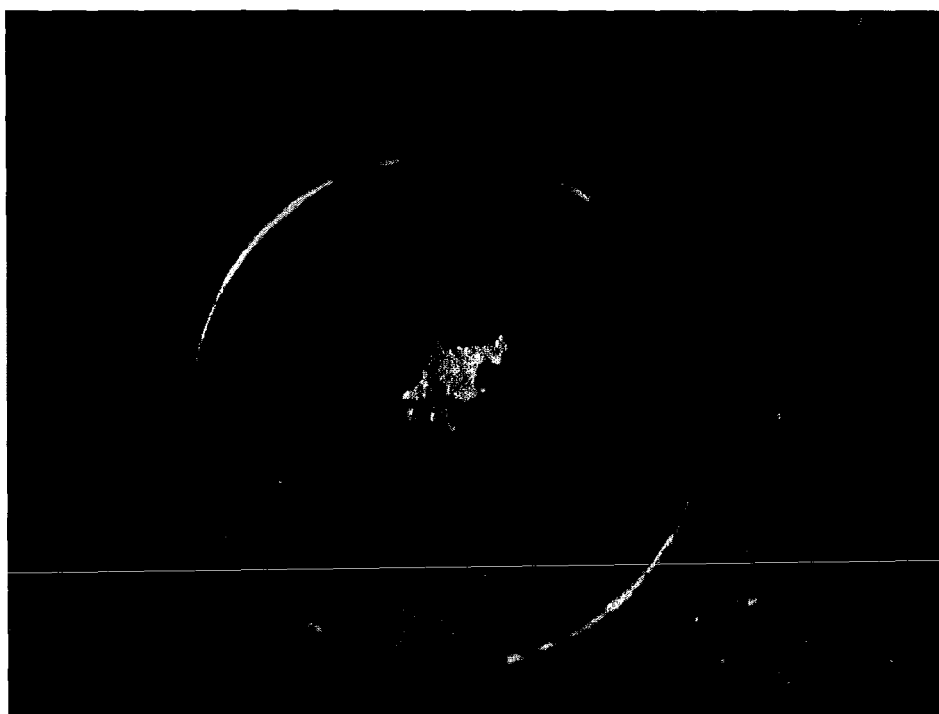


**Figure 5.10:** Melt prepared diamine crosslinked HBPE-g-MAH, after finding the degree of gelation using a Soxhlet apparatus; 70% of the resultant polymer was gelled.

#### 5.4 Conclusion

Solution amination of HBPE-g-MAH using 1,8-diaminooctane elucidated that the degree of crosslinking is independent of temperature beyond 120 °C and of reaction time. A reaction time of 1 hr is sufficient to achieve complete reaction between HBPE-g-MAH and diamine.

A critical concentration of 4 mol 1,8-diaminooctane/ mol HBPE-g-MAH gave the highest degree of crosslinking. Higher diamine concentrations resulted in decreased degree of crosslinking because of free amine attachment to the HBPE-g-MAH becoming the dominant reaction, as opposed to coupling between two chains, forming crosslinks.

The structure of the polymer was found to have tremendous effect on the concentration of diamine necessary to gel the polymer. The hyperbranched and globular nature of HBPE-g-MAH restricted accessibility of maleic anhydride moieties and diamine diffusion, and hence a higher concentration of diamine was needed to crosslink the polymer compared to that needed to crosslink PP-g-MAH in the work of Lu et al (8).

Melt amination of HBPE-g-MAH was successful, where a soft solid polymer was formed from two liquid reactants at 180 °C. This suggests that HBPE-g-MAH proved to be a potential material for reaction injection molding applications.

## 5.5 References

- (1) Rogerson, M. (2005). *What is crosslinked polyethylene and why do we use it?* MICROPOL: Retrieved April 26, 2008, from <http://www.pexassociation.com/warehouse/6/What%20is%20crosslinked%20polyethylene.pdf>
- (2) Thermo Fisher Scientific Inc. (2008). *Introduction to Crosslinking*. Retrieved April 26, 2008, from <http://www.piercenet.com/Products/Browse.cfm?fldID=CE4D6C5C-5946-4814-9904-C46E01232683>
- (3) Bayer MaterialScience LLC. (2008) *What's RIM?* Retrieved April 27, 2008, from <http://www.rimmolding.com/rim/index.html>
- (4) Creative Urethanes, Inc. (2008). *Reaction Injection Molding (RIM)*. Retrieved April 17, 2008, from [www.creativeurethanes.com/reactioninjectionmoldingrim.html](http://www.creativeurethanes.com/reactioninjectionmoldingrim.html)
- (5) Bayer MaterialScience LLC. (2008) *Advantages - Reaction Injection Molding (RIM)*. Retrieved April 27, 2008, from [www.rimmolding.com/rim/advantages.html](http://www.rimmolding.com/rim/advantages.html)
- (6) D 2765-95, *Test Methods for Determination of Gel Content and Swell Ratio of Crosslinked Ethylene Plastics*, Annual Book of ASTM Standards. 2006
- (7) De Roover, B.; Scalvons, M.; Carlier, V.; Devaux, J.; Legras, E.; Momtaz, A. J. *Polym Sci: Polym. Chem.* 1995, 33, 829
- (8) Lu, Q.-W.; Macosko, C.; Horriion, J. J. *Polym. Sci: Polym. Chem.* 2005, 43, 4217
- (9) PolymerProcessing. (2006). *Operations - Reaction Injection Molding*. Retrieved April 29, 2008, from <http://www.polymerprocessing.com/operations/rim/index.html>

## **Chapter 6: Significant Research Contributions and Recommendations for Future Developments**

### 6.1 Significant Research Contributions of Thesis Work

The following research work falls under the umbrella of polyolefin modification, in specific; this thesis concentrates on the peroxide initiated grafting of hyperbranched polyethylene with a monomer, namely, maleic anhydride, to improve compatibility and adhesion to polar substrates. In addition, to gain fundamental understanding through characterization and correlation of the reactions which take place. A number of significant conclusions and contributions to the polyolefin research field have been made in this thesis work; these contributions are respectively summarized as follows.

In Chapter 2, the reactions undergone by hyperbranched polyethylene modified by peroxide initiation are presented, by correlation to the zero shear viscosity data obtained from rheological characterization and to the number of CH, CH<sub>2</sub>, and CH<sub>3</sub> groups obtained from high-temperature <sup>13</sup>C-NMR experiments. Comparison to other commercially available polyolefins in terms of reactions such as crosslinking and degradation undergone upon modification are also presented. Studies have shown that hyperbranched polyethylene undergoes both crosslinking and degradation; however, it was found that degradation is the dominant reaction.

In Chapter 3, a novel material was prepared by grafting hyperbranched polyethylene with maleic anhydride; grafting was confirmed using FTIR and high temperature <sup>1</sup>H-NMR. The effect of process conditions and parameters, such as reaction

temperature, initiator concentration, monomer concentration, initiator type, and reaction time, on the grafting reaction was investigated, where a maximal grafting density of 1.7% was achieved using 2 wt.% DCP and 2 wt.% MAH, while running the reaction at 130 °C for 1 hr. Moreover, upon polymer grafting, a significant decrease in the water contact angle was attained in comparison to hyperbranched polyethylene, which is hydrophobic.

In Chapter 4, the rheological properties of hyperbranched polyethylene grafted with maleic anhydride were presented and compared to those of the parent polymer (hyperbranched polyethylene). Studies elucidated that hyperbranched polyethylene grafted with maleic anhydride exhibited a Newtonian behavior and showed a pure viscous response between 25 and 65 °C, analogous to hyperbranched polyethylene. However, an overall increase in viscosity, and a slight shear thinning behavior was noticed in the high shear rate region at low temperatures. It was concluded that grafting with maleic anhydride had no effect on the globular microstructure of the polymer.

In Chapter 5, crosslinking of hyperbranched polyethylene grafted with maleic anhydride was achieved using a diamine, and confirmed using FTIR. The effect of various process parameters such as reaction temperature, diamine concentration, and reaction time on the degree of crosslinking was examined; a maximal degree of crosslinking of 62.7% was achieved using 4 mol diamine/ mol HBPE-g-MAH. It was concluded that the structure of the polymer has immense effect on the concentration of

diamine required to gel the polymer. Nonetheless, melt amination of hyperbranched polyethylene grafted with maleic anhydride was successful; a solid gelled polymer was formed from viscous oil. This renders it as a type of potential material for reaction injection molding applications.

## 6.2 Recommendations for Future Research

### 6.2.1 Melt Grafting of Hyperbranched Polyethylene

Although solution grafting of maleic anhydride onto hyperbranched polyethylene was successful in this thesis, however, melt grafting through reaction extrusion is more industrially appealing as it is a continuous process with short reaction time and low infrastructure cost, which involves no use of solvent, and therefore simple product isolation. Investigation of melt grafting was not feasible in this work, due to the limited amount of hyperbranched polyethylene supplied, however, as a future development, melt grafting of hyperbranched polyethylene should be investigated. Success of melt grafting, will be of significant academic importance and industrial interest.

### 6.2.2 Mechanical Testing and Characterization of Crosslinked HBPE-g-MAH

This thesis work presented the successful crosslinking of HBPE-g-MAH, where a solid product was formed from very viscous oil. Larger scale preparation of this crosslinked product should be done in future work, enough for rheological and mechanical testing to be conducted, in order to have a better fundamental understanding of the microstructure of the gelled polymer, and to open the door for further

improvements to its properties through the addition of coagents and additives during the preparation process.

### 6.2.3 Reaction Injection Molding of crosslinked HBPE-g-MAH

Applicability of reaction injection molding technique in the preparation of diamine crosslinked HBPE-g-MAH should be investigated; this development can only be achieved through collaboration with an industrial partner. A great technological advancement will take place if this type of material can be prepared by reaction injection molding, which in turn will create a new area of industrial research that will further lead to the development of unique and specialized products and applications.